PLAINTIFF'S EXHIBIT

CAP-1815

A/C Pipe
Producers Association

Internal Correspondence

TO Public Affairs Committee
International Affairs Committee

FROM J. F. Welch
J. F. Welch, Vice President

DATE February 10, 1982

SUBJECT U.S. Environmental Protection Agency (EPA) - Research on Corrosion of A/C Water Pipe

ACTION REQUIRED: Review for information

Enclosed is an article, "The Behavior of Asbestos Cement Pipe Under Various Water Quality Conditions: Part 2, Theoretical Considerations" by Schock and Buelow. This report summarizes the most recent results of EPA's research on the corrosion of A/C pipe. Beyond the theoretical considerations of complexation and solubility equilibria, the most important finding is that the Aggressiveness Index (AI) as well as other indices of water corrosivity are

> ... not theoretically sound from a chemical standpoint to predict fiber release and degradation of the interior surface in systems that are undersaturated with respect to calcite. Fortunately, it (AI) has generally proved to predict falsely pipe deterioration more often than to predict falsely pipe stability in field situations.

The report goes on to state that "natural inhibitory factors" such as the presence of iron, manganese, silica and organic matter may bind asbestos fibers even though the pipe surface is softened from corrosive water attack.

The finding with the most potential negative impact follows:

> The results of DWRD experiments conducted thus far and field observations indicate that addition of the corrosion-control compounds tested thus far cannot be relied upon to provide correction of A/C pipe deterioration.

Advocates of the regulation of A/C pipe now may say that its use should be restricted because once deterioration ("surficial softening from aggressive water") begins, it is irreversible and consumer exposure to asbestos in drinking water will be continuous.

In many respects, however, this research supports the conservatism of the Aggressive Index or Langelier Saturation Index as suitable criteria for predicting the long term structural integrity of A/C water pipe. Moreover, it bolsters the industry's long held opinion that the only accurate means to determine whether an A/C water system is releasing asbestos fibers is to ensure that manufacturing or construction asbestos residues are thoroughly flushed and accurate asbestos in water analyses taken. Corrosion indices along will not suffice.

If you have any questions, please do not hesitate to call.

JFW/ajb

Enclosure

cc: A. Kahn, Esq.
N. Rahn, Esq.
Asbestos International Association
Asbestos Institute
Special Counsel (Cal., Ariz., Texas, Conn.)
Brian Commins, Ph.D.
Kirkland & Ellis

copies to:

Public Affairs Committee

H. Olson
B. Cook
R. LeGault
W. Perrell
J. Woods
J. Baker
T. Dougherty
D. Stinson
W. McCallie
B. Collier

International Affairs Committee

R. Dorner
E. van der Rest
B. Giboin
N. Officer
R. Hobbs
A. Saoulis
R. Jalan
V. Pattabhi
H. Hudson
C. Barton
S. Al-Tarkait

H01PI20902
Chrono

RESEARCH AND TECHNOLOGY

The behavior of asbestos-cement pipe under various water quality conditions: Part 2, theoretical considerations

Michael R. Schock and Ralph W. Buelow

A water chemical model involving the complexation and solubility equilibria of calcium, magnesium, zinc, iron, manganese, silica, chloride, orthophosphate, and carbonate has been developed and applied to laboratory pipe-loop-coupon and field data on asbestos-cement pipe. Calculation of the saturation states of the relevant solids enables graphic guides to be prepared for the prediction of dosage levels for in-situ pipe coating by zinc compounds as well as protection afforded by coatings formed by natural inhibitory constituents of the water.

Because of concern about the possible problem of asbestos fibers being released from the walls of asbestos-cement (A-C) pipe, the AWWA Research Foundation reviewed the problem and in September 1974[1] suggested several research needs in this area. As a response to this call for research, several projects were designed by the US Environmental Protection Agency, Drinking Water Research Division (DWRD), to determine whether A-C pipe would be attacked and asbestos fibers would be released from the pipe under various conditions of water quality. In general, this research has been divided into four phases: first, a field evaluation of 10 public water supply systems that used A-C pipe; second, an A-C pipe-loop system operated under controlled conditions; third, several tests of A-C "pipe coupons"; and fourth, two field research projects that are attempting to rehabilitate deteriorated pipe in place. Part 1 of the project report[2] contained the experimental results of the first three of these four phases. Additional research by DWRD into various methods of analytical determination, primarily by microscopy, has been reported.[3]

This paper relates to the A-C pipe coupon tests reported in part 1, particularly the studies of the protection of the A-C pipe against attack from aggressive waters. Table 1 shows the water quality of most of the DWRD recirculation experiments (as of July 1980) concerned with A-C pipe protection. Table 2 summarizes the qualitative results of the 16 DWRD laboratory experiments referred to later in this paper.

This paper examines the solution interactions that were seen to govern the effectiveness of the zinc compounds as corrosion inhibitors. The model developed is then extended to show how similar considerations of the aqueous equilibria of other metals and nonmetals may be used to predict more effectively the true aggressiveness of a water toward A-C pipe in actual distribution systems.

Critique of the "Aggressiveness Index"

Classically, the tendency of a water to deteriorate the structure of asbestos-cement pipe has been described by the "Aggressiveness Index" (AI),[4,5] given as

$$AI = pH + \log (AH)$$

where $pH = -\log aH^+$ (−log of the hydrogen ion activity); A = total alkalinity in mg/L as $CaCO_3$; and H = calcium concentration in mg/L as $CaCO_3$.

Waters possessing an AI equal to or exceeding 12.0 are considered to be "nonaggressive"; those with an $AI \leq 10.0$ are said to be "highly aggressive"; and those with an AI between 10 and 12 are "moderately aggressive." The AI is derived[5] from a simplified form of the Langelier Index of calcite saturation[5,7] with factors introduced to compensate for the temperature dependency of the solubility product constant (K_{s0}) of calcite and for the ionic strength[5,9] of the solution.

The factors for temperature and ionic strength compensation utilized in the derivation of the 12.0 value of[5] the AI correspond to a temperature of approximately 14°C and an ionic strength of

0003-150X/81/120636-16$02.00

TABLE 1
Water qualities of DWRD recirculation experiments

Experiment Number	pH	Total Alkalinity mg/L as $CaCO_3$	Ca mg/L	Zn mg/L	PO_4 mg/L	Na mg/L	K mg/L	Mg mg/L	SiO_2 mg/L	Cl mg/L	FCR† mg/L as Cl	TDS mg/L	SPC μS/cm	AI‡	Treatment Chemical
1	8.2	20-27	5-13								0.1-0.4	30-60		10.2-10.8	none
2	8.2	20-26	4-8	0.3-0.5	0.4-1						0.1-0.4	32-61		10.1-10.5	zinc orthophosphate§
3	7.0	21-25	10-22								0.1-0.4	45-71		9.3-9.7	none
4	7.0	20-29	9-17	0.3-0.6	0.4-1						0.1-0.4	49-72		9.3-9.7	zinc orthophosphate§
5	8.2	19-22	5-8	0.3-0.7					0.1-2		0.1-0.4	36-41		10.2-10.4	zinc chloride
6	7.5	116-130	133-155	0.03		60**			1-4	94**	0-0.6	340-360		11.7-11.8	none
7	7.9	120-131	129-160	0.04		60**			1-4	94**	0-0.7	330-350		12.1-12.2	$CaCl_2/NaHCO_3$
8	9.0	38-42	21-30	<0.02					0.1-2		0-0.4	80-101		11.9-12.1	$CaCl_2/NaHCO_3$
9	8.2	42-50	9-16	0.02	0.2				15-16	30	0.1-0.5	148	231	10.8-11.1	sodium metasilicate
10††	7.0	25-27	13-16	0.1				1.5	14-17		0-0.5	108		9.3-9.6	sodium metasilicate
11	8.2	18-19	0.6-4	0.3-0.4	0.03	10	<0.1	0.1	3	<10	0.2-0.6	24		9.2-10.1	zinc chloride
12	7.5	18-21	9-14	0.3-0.4	0.03	8-9	0.2	0.6	2-3	<10	0.2-0.5	41	78	9.7-10.0	zinc chloride
13	8.2	19-21	10-15	0.1-0.2	0.03	9-10	0.2	0.6	0.2	<10	0.2-0.5	44	83	10.5-10.7	zinc chloride
14	8.2	2-6	32-43	0.3-0.4	0.06			1.3	1-8	27	0.2-0.6	83	104	10.0-10.4	zinc chloride
18	8.2	16-19	7-10	0.3-0.5	<0.2	13		0.8	<0.4	<10	0.4-0.7	47-63	100	10.2-10.5	zinc sulfate
19	7.2	18-21	9-25	0.1	0.1	10	0.3	1.0	<0.2	13	0.1-0.3	43	78	9.4-9.9	zinc chloride and iron (III) chloride

*Analyses represent concentrations at or near the end of each experiment unless a range is given. All sulfate values were less than the 15-mg/L detection limit. Based on the water blending conditions, the probable range was 5-10 mg/L. Iron was less than the 0.1 mg/L calibration limit, except for experiment 19 in which approximately 0.1 mg/L of iron was added.

†Free chlorine residual measured one week after each dose

‡AI = Aggressiveness Index range; see text for definition

§Virchem 931, a product of Virginia Chemical Corp., Portsmouth, Va.

**Sodium and chloride concentrations are estimated from reagent additions. There was a large analytical scatter on the calcium and total alkalinity results.

††The same coupon was previously run for almost one month at SiO_2 concentration of 10-30 mg/L and zinc approximately equal to 0.2 mg/L at a similar pH, total alkalinity, and calcium level.

proximately 0.01. The solubility product constant for calcite was apparently taken from the work of Larson and Buswell.[7] The intent of the AI, when originally conceived, was to indicate environments that would tend to damage the structural integrity of the pipe.

There are several major avenues by which the AI is open to criticism as an indicator of corrosivity and fiber release, the manner in which it has most frequently been used. The foremost problem is that the derivation of the AI is based on the Langelier Index of calcium-carbonate saturation with some approximate adjustments for temperature and ionic strength.[5] Insofar as the A-C pipe would indeed be protected by a coating of $CaCO_3$ if active $CaCO_3$ precipitation were occurring, the AI would then give a fairly accurate prediction of nonaggressiveness. However, in the case of calcium-carbonate undersaturation, the aggressiveness of the water toward the pipe will be dictated by other chemical equilibria. Calcium carbonate is, at maximum, a trivial component of the matrix of A-C pipe;[10] therefore, there is no a priori reason to expect the AI as traditionally conceived to give an accurate prediction of the pipe's interior surface condition in waters undersaturated with respect to calcite.

A second criticism relates to the solubility product constant of calcite used in the derivation of the index. Work by Langmuir,[11] Jacobson and Langmuir,[12] and Christ et al[13] not only corrects for ion-pairing effects not considered previously[7] during solubility experiments but also indicates that the quantitative temperature dependency of K_{s0} found by Larson and Buswell[7] is erroneous, particularly in the range of 0 to 15°C, a common range for natural and drinking waters. The higher value of K_{s0} given by Larson and Buswell[7] probably results primarily from ignoring the ion pairs; to the extent that few environmental workers have applied such corrections to field and laboratory data, the error in K_{s0} has not been obvious. Also, a metastable $CaCO_3$ phase of considerably higher solubility than calcite is probably the initially precipitated form of $CaCO_3$ in soil root zones[14] and in water treatment.[15] Precipitation of aragonite, which is more soluble than calcite, in lake marls and marine environments has been commonly observed.[14] The occurrence of mixed precipitates of calcite and aragonite, as well as the stabilization of aragonite relative to calcite by such ions as Mg^{2+}, Sr^{2+}, trace levels of Zn^{2+}, and some organic materials, has been documented.[16-18] A similar phenomenon probably takes place in drinking water. Therefore, those studying calcium-carbonate precipitation may tend to regard the Larson and Buswell constant,[7] which predicts higher solubility for calcite, as being closer to observation and therefore more correct, rather than noting its thermodynamic questionability and seek further explanation.

The simple expedient of making temperature and ionic-strength adjustments by averaging a range of values of temperature and total dissolved solids may result in more correct approximations in some cases, but it is an inherent source of error and uncertainty in other cases. When attempts are made to predict the amount of pipe softening or calcium leaching from the pipe interior by using the AI of the water, additional error is introduced by implying a correlation between the magnitude of calcite undersaturation and the rate of dissolution of the predominantly calcium-silicate pipe. A correlation between faster calcium leaching and greater calcite undersaturation is, more probably, a coincidence resulting from some kinetic effect of calcium concentrations in the waters (and probably the pH) with regard to calcium-silicate or calcium-hydroxide saturation.

Later in this paper the AI will be shown to be further deficient in reliably predicting the A-C pipe condition, because it

TABLE 2
Summary of qualitative results of DWRD A/C pipe treatment experiments

Experiment Number	pH	Treatment Process	Inner Wall of Coupon Softened?
1	8.2	none	yes
2	8.2	zinc (orthophosphate) 0.3–0.5 mg/L	no
3	7.0	none	yes
4	7.0	zinc (orthophosphate) 0.3–0.5 mg/L	slightly
5	8.2	zinc (chloride) 0.3–0.7 mg/L	no
6	7.5	none	yes
7	7.9	$CaCO_3$ saturation	very slightly
8	9.0	$CaCO_3$ saturation	slightly
9	8.2	sodium metasilicate	no
10	7.0	sodium metasilicate	no
11	8.2	zinc (chloride) 0.4 mg/L; low calcium	no
12	7.5	zinc (chloride) 0.4 mg/L	slightly
13	8.2	zinc (chloride) 0.1–0.2 mg/L	yes
14	8.2	zinc (chloride) 0.4 mg/L; low alkalinity	very slightly
16	8.2	zinc (sulfate) 0.5 mg/L	no
19	7.2	iron (III) (chloride) 0.1 mg/L; zinc (chloride) 0.1 mg/L	slightly

TABLE 3
Aqueous species considered in saturation index and solubility diagram preparation

Species	
H^+	$ZnCl_2^\circ$
OH^-	$ZnCl^+$
$H_2CO_3^\circ$	$ZnCl_3^-$
HCO_3^-	$ZnClOH^\circ$
CO_3^{2-}	$ZnHPO_4^\circ$
$H_3PO_4^\circ$	$ZnH_2PO_4^+$
$H_2PO_4^-$	$ZnOH^+$
HPO_4^{2-}	$Zn(OH)_2^\circ$
PO_4^{3-}	$Zn(OH)_3^-$
Ca^{2+}	$Zn(OH)_4^{2-}$
$CaHCO_3^+$	Zn_2OH^{3+}
$CaCO_3^\circ$	Fe^{3+}
$CaHPO_4^\circ$	$FeOH^{2+}$
$CaPO_4^-$	$Fe(OH)_2^+$
$CaH_2PO_4^+$	$Fe(OH)_3^\circ$
$CaOH^+$	$Fe(OH)_4^-$
Mg^{2+}	$Fe_2(OH)_2^{4+}$
$MgHCO_3^+$	$Fe_3(OH)_4^{5+}$
$MgOH^+$	$FeSO_4^+$
$MgCO_3^\circ$	$FeCl^{2+}$
$MgHPO_4^\circ$	$FeCl_2^+$
Na^+	$FeCl_3^\circ$
$NaCO_3^-$	$FeHPO_4^+$
$ZnCO_3^\circ$	
$ZnCl^+$	

TABLE 4
Solid species considered in Saturation Index and solubility diagram preparation

Solid (Chemical Formula)	Common Name
$CaCO_3$	calcite
$Ca(OH)_2$	portlandite
$CaHPO_4 \cdot 2H_2O$	brushite
$Ca_8H_2(PO_4) \cdot 5H_2O$	octacalcium phosphate
$Ca_5(PO_4)OH$	hydroxyapatite
$MgCO_3$	magnesite
$Mg(OH)_2$	brucite
$Mg_3(PO_4)_2$	magnesium orthophosphate
$ZnCO_3$	smithsonite
$Zn_5(OH)_6(CO_3)_2$	hydrozincite
$Zn(OH)_2$	zinc hydroxide
$Zn_3(PO_4)_2 \cdot 4H_2O$	a-hopeite
$Fe(OH)_3$	amorphous iron (III) hydroxide
$FePO_4 \cdot H_2O$	strengite

fails to take into account protective chemical reactions in drinking water aside from calcite deposition.

Mechanism of A-C pipe dissolution

Attack on A-C pipe by drinking water manifests itself as deterioration of the interfacial fraction of the interior pipe surface, which can lead to the release of asbestos fibers, about which there is considerable concern for possible human health effects.[19,20] Field and laboratory observations by DWRD have shown that sometimes adherent coatings form on the pipe that will prevent fiber release, but which may or may not totally prevent some surficial softening. The cement matrix of A-C pipe is a very complicated combination of compounds and phases, some of which are poorly identified or are of indefinite composition. More than 100 compounds and phases important to the chemistry of portland and related cements have been described and identified,[21] and because of solid solution possibilities, probably many more exist. The state of knowledge of the thermodynamic solubilities in water of the individual predominant compounds of the cement lags far behind that of minerals and related man-made compounds important to drinking water chemistry. Until more research is done, only some qualitative generalizations can be made.

The corrosion of A-C pipe is governed almost completely by solubility considerations. Thus, the dissolution and coating processes of the pipe may be described and predicted by bulk-solution chemical parameters and straightforward solid solubility reactions.

The effects of pipe dissolution on the distribution system water quality, in addition to fiber release, are several.

The "free-lime" component of the pipe (essentially equivalent to the solid portlandite) can dissolve as represented by the reaction

$$Ca(OH)_2(s) = Ca^{2+} + 2OH^- \quad (1)$$

for which K_{s0} is $10^{-5.20}$. This would increase the pH, titration alkalinity, and the calcium content of the water (and, therefore, the AI) during its passage through the pipe. The pH increase would enhance the ability of the water to absorb and hydrate any CO_2 gas present. Subsequently, the reaction of any absorbed CO_2 with the hydroxyl ions present would lead to the formation of bicarbonate ions, a step that would favor increased dissolution of $Ca(OH)_2(s)$ by the mass-action effect. In the present commercial autoclaved type II A-C pipe, the free-lime phase is ≤ 1.0 percent by weight.[4]

Three of the predominant crystalline phases of the matrix of A-C pipe are tricalcium silicate (nominally Ca_3SiO_5), dicalcium silicate (nominally Ca_2SiO_4), and tricalcium aluminate ($Ca_3Al_2O_6$).[10,21] Possible dissolution reactions may be represented by

$$Ca_3SiO_5(s) + 5H_2O = 3Ca^{2+} + H_4SiO_4^\circ + 6OH^- \quad (2)$$

$$Ca_2SiO_4(s) + 4H_2O = 2Ca^{2+} + H_4SiO_4^\circ + 4OH^- \quad (3)$$

$$Ca_3Al_2O_6(s) + 6H_2O = 3Ca^{2+} + 2Al^{3+} + 12OH^- \quad (4)$$

Estimates of the solubility constants for reactions (2) and (3) were obtained by using an internally consistent set of Gibbs free energy of formation data[22] at 25°C and, at 101 kPa (1 atm) pressure, are $10^{-8.5}$ and 10^{-18}, respectively. Free-energy data have thus far not been located for $Ca_3Al_2O_6$. Since there is still considerable uncertainty as to the exact crystal structure of this solid,[21] lack of thermodynamic characterization would not be surprising.

Because solids are often highly substituted in portland cement[21], their true thermodynamic activities may be somewhat different from unity.[23,24] Therfore, either the free energies tabulated may not exactly correspond to conditions in cement, or the activity of the solid may need to be included in the solubility constant expression if it is used to determine

... the solids tricalcium silicate ...nd dicalcium silicate are highly soluble ...nder general drinking water conditions. ...eactions of other solid phases can also ...asily mobilize sodium and potassium.

Dissolution by reactions of the type of [2], [3], and [4], even if the estimated solubility constants are not very accurate, would produce three major effects. First, the levels of calcium, aluminum, and silicon species (as well as any substitutional elements) will increase with time upon standing, or with distance of passage through a pipeline, unless threshold conditions are met for saturation and precipitation of another less soluble phase, or until the available supply of leachable species is depleted for a given depth of penetration.

Second, the pH of the system would tend to increase because of several dissolution reactions and the two dissociations of silicic acid.[25] The overall solution pH may also be increased slightly by dissolution of the asbestos fibers themselves. For example, the overall process of chrysotile-fiber dissolution as given by the equation

$$Mg_3Si_2O_5(OH)_4(s) + 5H_2O \rightleftharpoons 3Mg^{2+} + 2Si(OH)_4^\circ + 6OH^- \quad (5)$$

would tend to increase the pH by virtue of the input of hydroxyl ion and soluble silicic into the water, because chrysotile has K_{s0} of -51.8,[26] but the total mass of ... involved is quite small.

...me hydrolysis of Al^{3+} ion introduced ...ng dissolution of tricalcium aluminate may take place, but field observations in distribution systems indicate the pH-increasing reactions are dominant.[2] Also, large pH gradients between pipe surface and the bulk solution would not normally be expected. The ... in a distribution main would have ...nal periods of suspended flow, such as a household system during overstanding, except at the dead ends. the buffer capacities of most, even ...sive, water should be sufficient to ...ntially moderate a pH rise, especially when such capacities are combined ...nstant water flow. Additionally, a ...rge local rise in pH would often ...$CaCO_3$ deposition and subsequent ...ion, a situation that tends to con... ...th the observation of continual ...ching in field and laboratory tests ...d in part 1[2] and later in this

... the alkalinity of the system may ...w an increase. Considering that ...y is a charge-neutralizing capac... only newly-formed directly... ...ting entities would be OH^-, ...$^-$, and $SiO_2(OH)_2^{2-}$. However, a ...ase favors the production of ...d CO_3^{2-}, normally the dominant ... in pure drinking water having a pH less than approximately 9 to 10. Importantly, the alkalinity increases observed in field studies[2] do not necessarily indicate input of dissolved carbonate from pipe materials. Carefully obtained, analyzed, and preserved samples for potentiometric total alkalinity, pH, temperature, and major constituents can be used to calculate changes in carbonate concentration.[23,26,27]

Protection by $CaCO_3$ saturation

Three experiments reported in part 1[2] (experiments 6, 7, and 8) evaluated the effectiveness of maintaining solution composition near to slightly above $CaCO_3$ (calcite) saturation by adjustment of calcium, total carbonate concentration (C_t), total alkalinity (Alk_t), and pH simultaneously. As would be expected, the pipe integrity was maintained with only a little softening when it was at the calcite saturation level[26] and with virtually no deterioration when it was slightly above.

The small amount of pipe softening observed in experiment 8 is not particularly surprising and may be explained by several factors. At least two of the major phases of portland cement, the primary matrix material of the pipe, are thermodynamically highly unstable in most drinking waters, as was shown earlier. Another factor is the role that pH plays in the attainment of $CaCO_3$ saturation.

A series of calculations, or the use of a graphic method such as a Caldwell-Lawrence diagram,[27,28] will show that a greater mass of $CaCO_3$ can be deposited at a low pH with high calcium and carbonate concentrations than at a high pH with low calcium and carbonate concentrations.

As was mentioned previously, the first-formed $CaCO_3$ precipitate (even if it is metastable) most probably is described by a more soluble K_{s0} than calcite. It is desirable to take this phenomenon into account, as well as complexation and ion pairing, when a conditioning scheme based on calcium-carbonate saturation is devised.

A more rigorous computation of the saturation conditions previously reported[2] for experiments 6, 7, and 8, was performed by means of the aqueous equilibrium calculation computer program WATSPEC2,[29] an enhanced version of WATSPEC.[30] All systems were calculated to be undersaturated with the estimated freshly precipitated phase[31] but were at or above saturation with calcite.

The calculated SI values suggest that experiment 6 should not have provided protection by calcium-carbonate deposition, and the coupon was seen to be considerably softened.[2] Experiments 7 and 8 were near the thermodynamic precipitation threshold for aragonite and a fresh precipitate. The analytical data are inconclusive as to whether or not active precipitation was actually taking place (evidenced by no clear decrease or leveling off of calcium or total carbonate concentrations). Increased stabilization of certain calcium-silicate phases of the pipe by the lower pH and higher calcium present in experiment 7 (as opposed to experiment 8) is an alternative possibility. The condition of the pipe coupons does support addition of calcium and carbonate to attain calcium-carbonate saturation at relatively low pH values as a viable protection strategy.

Though protection by calcium-carbonate saturation is a well-established corrosion-inhibition technique, the expense of the treatment chemicals for water supplies of low hardness and alkalinity, as well as the undesirability to many consumers of the harder water then obtained, makes finding other alternative treatment methods an attractive endeavor.

Protection by metal precipitation

Just as calcium carbonate may precipitate and adhere to a pipe surface to form a protective coating, so too could any other reasonably dense solid. Unfortunately (from this standpoint), few combinations of cations and anions are present in drinking water in sufficient quantity to provide enough mass for precipitation and effective pipe coating. Four elements that can form useful coatings are iron, zinc, manganese, and silicon.

The first purpose of this section is to use computer calculations of chemical equilibria in hypothetical model systems to develop a predictive model of aggressive and nonaggressive water conditions. A second purpose is to show by correlation of the computer model with field data and laboratory experiments that the true aggressiveness of drinking waters with respect to A-C pipe can be predicted more accurately than by using the AI alone. Situations that are in conflict with the AI most probably are not anomalous phenomena but result from shortcomings in the chemical basis of the index that render it an ineffective predictive tool. Finally, this section will show how the model may be used to devise protective or corrective treatment conditions.

Calculation methodology. The model systems considered were chosen mainly to approximate laboratory experiments (completed or planned) or to illustrate some possible field situations. Obviously, not all combinations of important variables could be covered; however, the general solution charcteristics covered by the example systems should enable them to be applied directly to most cases not specifically shown.

The models were calculated by utilizing the aqueous equilibrium modeling program REDEQL.EPAK[31,32] written in the FORTRAN IV language and run on an

TABLE 5
Aqueous reactions considered in the construction of the Saturation Index and precipitation diagrams

Reaction	log Kt	Source
Hydrogen		
$H^+ + OH^- = H_2O$	14.00	1
$2H^+ + CO_3^{2-} = H_2CO_3^*$	16.7	2
$H^+ + CO_3^{2-} = HCO_3^-$	10.3	3
$2H^+ + CO_3^{2-} = CO_2(g) + H_2O$	18.14	2
$H^+ + PO_4^{3-} = HPO_4^{2-}$	12.4	4
$2H^+ + PO_4^{3-} = H_2PO_4^-$	19.6	4
$3H^+ + PO_4^{3-} = H_3PO_4^*$	21.7	4
Calcium		
$Ca^{2+} + H_2O = CaOH^+ + H^+$	−12.6	5
$Ca^{2+} + CO_3^{2-} = CaCO_3^*$	3.2	5
$Ca^{2+} + CO_3^{2-} + H^+ = CaHCO_3^+$	11.3	5
$Ca^{2+} + H^+ + PO_4^{3-} = CaHPO_4^*$	15.1	5
$Ca^{2+} + 2H^+ + PO_4^{3-} = CaH_2PO_4^+$	20.3	5
$Ca^{2+} + PO_4^{3-} = CaPO_4^-$	6.5	5
Magnesium		
$Mg^{2+} + H_2O = MgOH^+ + H^+$	−11.8	5
$Mg^{2+} + CO_3^{2-} = MgCO_3^*$	3.0	5
$Mg^{2+} + CO_3^{2-} + H^+ = MgHCO_3^+$	11.4	5
$Mg^{2+} + H^+ + PO_4^{3-} = MgHPO_4^*$	15.3	5
Sodium		
$Na^+ + CO_3^{2-} = NaCO_3^-$	1.2	5
Zinc		
$2Zn^{2+} + H_2O = Zn_2OH^{3+} + H^+$	−9.0	1
$Zn^{2+} + H_2O = ZnOH^+ + H^+$	−8.0	1
$Zn^{2+} + 2H_2O = Zn(OH)_2^* + 2H^+$	−16.9	1
$Zn^{2+} + 3H_2O = Zn(OH)_3^- + 3H^+$	−28.4	1
$Zn^{2+} + 4H_2O = Zn(OH)_4^{2-} + 4H^+$	−41.2	1
$Zn^{2+} + H^+ + PO_4^{3-} = ZnHPO_4^*$	15.6	4
$Zn^{2+} + 2H^+ + PO_4^{3-} = ZnH_2PO_4^+$	21.2	4
$Zn^{2+} + CO_3^{2-} = ZnCO_3^*$	4.8‡	6
$Zn^{2+} + H_2O + Cl^- = ZnClOH^+ + H^+$	−7.5	7
$Zn^{2+} + Cl^- = ZnCl^+$	0.4	4
$Zn^{2+} + 2Cl^- = ZnCl_2^*$	0.6	4
$Zn^{2+} + 3Cl^- = ZnCl_3^-$	0.5	4
$Zn^{2+} + 4Cl^- = ZnCl_4^{2-}$	0.2	4
Iron		
$Fe^{3+} + H_2O = FeOH^{2+} + H^+$	−2.2	1
$Fe^{3+} + 2H_2O = Fe(OH)_2^+ + 2H^+$	−5.7	1
$Fe^{3+} + 3H_2O = Fe(OH)_3^* + 3H^+$	−13.6	1
$Fe^{3+} + 4H_2O = Fe(OH)_4^- + 4H^+$	−21.6	1
$2Fe^{3+} + 2H_2O = Fe_2(OH)_2^{4+} + 2H^+$	− 3.0	1
$3FE^{3+} + 4H_2O = Fe_3(OH)_4^{5+} + 4H^+$	− 6.3	1
$Fe^{3+} + H^+ + PO_4^{3-} = FeHPO_4^+$	17.8	5
$Fe^{3+}Cl^- = FeCl^{2+}$	1.4	5
$Fe^{3+} + 2Cl^- = FeCl_2^+$	2.1	5
$Fe^{3+} + 3Cl^- = FeCl_3^*$	1.1	5

†All data are for 25°C.
‡The published data of Bilinski et al[6] have been reinterpreted by Schock et al[7] in terms of both $ZnCO_3^*$ and $Zn(CO_3)_2^{2-}$, with log K = 5.2 for $ZnCO_3^*$ and with log K = 7.5 for the reaction: $Zn^{2+} + 2CO_3^{2-} = Zn(CO_3)_2^{2-}$. These constants were incorporated into the model after the calculations reported in this paper were performed.
Sources:
1. BAES, C.F. JR. & MESMER, R.E. *The Hydrolysis of Cations*, Wiley-Interscience, New York (1976).
2. HARNED, H.S. & DAVIES, R. JR. *Jour. ACS*, 65:2030 (1943).
3. HARNED, H.S. & SCHOLES, S.R. JR. *Jour. ACS*, 63:1706 (1941).
4. SMITH, R.M. & MARTELL, A.E. *Critical Stability Constants: Vol. 4, Inorganic Complexes*. Plenum Press, New York (1976).
5. PLUMMER, L.N. ET AL. WATEQF—A FORTRAN IV Version of WATEQ, A Computer Program for Calculating Chemical Equilibrium of Natural Water. USGS WRI 76-13 (Dec. 1978).
6. BILINSKI, H. ET AL. *Anal. Chim. Acta*, 84:157 (1976).
7. WAGMAN, D.D. ET AL. NBS Tech. Note 270-3 (Jan. 1968).

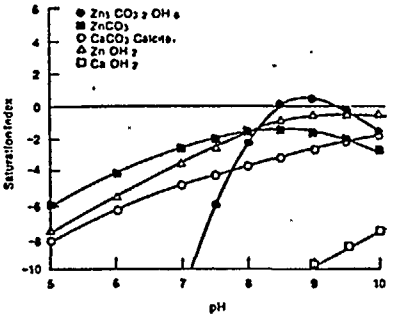

Figure 1. Saturation Index diagram for model system M1

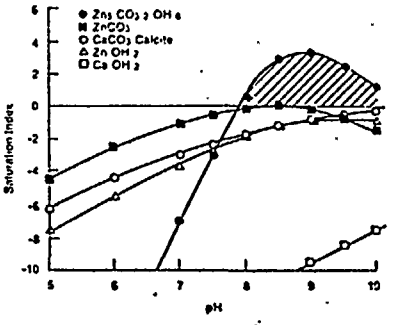

Figure 2. Saturation Index diagram for model system M8

TABLE 6
*Solid reactions considered in Saturation Index diagram preparation**

Reaction	log K	Source
Calcium		
$Ca^{2+} + CO_3^{2-} = CaCO_3(s)$	8.5	1
$Ca^{2+} + 2H_2O = Ca(OH)_2(s) + 2H^+$	−22.8	2
$Ca^{2+} + H^+ + PO_4^{3-} + 2H_2O = CaHPO_4 \cdot 2H_2O(s)$	18.9	3
$8Ca^{2+} + 6PO_4^{3-} + 2H^+ + 3H_2O = Ca_8H(PO_4)_3 \cdot 3H_2O$	46.9	3
$5Ca^{2+} + 3PO_4^{3-} + H_2O = Ca_5(PO_4)_3OH(s) + H^+$	40.6	4
Magnesium		
$Mg^{2+} + CO_3^{2-} = MgCO_3(s)$	7.5	5
$Mg^{2+} + 2H_2O = Mg(OH)_2(s) + 2H^+$	−16.8	7
$3Mg^{2+} + 2PO_4^{3-} + 8H^+ = Mg_3(PO_4)_2 \cdot 8H_2O(s)$	25.2	2
Zinc		
$Zn^{2+} + CO_3^{2-} = ZnCO_3(s)$	10.8	6
$5Zn^{2+} + 2CO_3^{2-} + 6H_2O = Zn_5(OH)_6(CO_3)_2(s) + 6H^+$	−9.7	6
$Zn^{2+} + 2H_2O = Zn(OH)_2(s) + 2H^+$	−12.5	7
$3Zn^{2+} + 2PO_4^{3-} + 4H_2O = Zn_3(PO_4)_2 \cdot 4H_2O(s)$	35.3	8
Iron III		
$Fe^{3+} + 3H_2O = Fe(OH)_3(s) + 3H^+$	−4.9	5
$Fe^{3+} + PO_4^{3-} + 2H_2O = FePO_4 \cdot 2H_2O(s)$	26.4	2

*All data are for 25°C.
Sources:
1. JACOBSON, R.L. & LANGMUIR, D. *Geochim. Cosmochim. Acta*, 38:301 (1974).
2. SMITH, R.M. & MARTELL, A.E. *Critical Stability Constants: Vol. 4, Inorganic Complexes*. Plenum Press (1976).
3. LINDSAY, W.L. & MORENO, E.C. *Soil Sci. Soc. Amer. Proc.*, 24:177 (1960).
4. MORENO, E.C. ET AL. *Jour. Res. NBS*, 72A:6:773 (Nov.-Dec. 1968).
5. PLUMMER, L.N. ET AL. USGS WRI 76-13. (Dec. 1978).
6. SCHINDLER, P. ET AL. *Helv. Chim. Acta*, 52:2327 (1969).
7. BAES, C.F. JR. & MESMER, R.E. *The Hydrolysis of Cations* Wiley-Interscience, New York (1976).
8. NRIAGU, J.O. *Geochim. Cosmochim. Acta*, 37:2357 (1973).

TABLE 7
*Model systems for zinc, iron (III), and calcium coating of A-C pipe at 25°C**

System	Calcium mg/L as Ca	Calcium mg/L as $CaCO_3$	Total Carbonate mg/L as CO_3	Total Carbonate mg/L as $CaCO_3$	Mg mg/L	Na mg/L	Cl mg/L	Zn mg/L	Fe mg/L	PO_4 mg/L	Figure[s]
M1	0.4	1.0	0.6	1.0	0.1	5	4-9	0.5	0	0	1
M2†	0.4	1.0	0.6	1.0	0.1	5	4-9	0.1	0	0	
M3	0.4	1.0	1.5	2.5	0.1	10	11-17	0.5	0	0	
M4	0.4	1.0	1.5	2.5	0	10	11-17	0	0.1	0	
M5†	0.4	1.0	6.0	10.0	0	10	8-17	0.1	0	0	
M6	0.4	1.0	12	20.0	1.0	12	9-23	0.5	0	0	
M7†	0.4	1.0	60	100.0	0.1	60	42-92	0.1	0	0	
M8	1.0	2.5	24	40.0	0.24	20	11-33	0.5	0	0	2,3
M8P	1.0	2.5	24	40.0	0.24	20	11-33	0.5	0	0.5	
M9	4.0	10.0	24	40.0	1.0	20	18-40	0.15	0	0	4,5
M10	4.0	10.0	12	20.0	1.0	12	15-29	0.5	0	0	6,7
M10P	4.0	10.0	12	20.0	1.0	12	15-29	0.5	0	0.5	
M11	4.0	10.0	12	20.0	1.0	12	15-29	0.3	0.1	0	8,9
M12	4.0	10.0	24	40.0	1.0	20	5-28	0.5	0	0	10,11
M12P	4.0	10.0	24	40.0	1.0	20	5-29	0.5	0	0.5	12,13
M13	4.0	10.0	60	100.0	1.0	30	4-56	0.5	0	0	14,15
M13P	4.0	10.0	60	100.0	1.0	30	4-56	0.5	0	0.5	16,17
M14	8.0	20.0	2.4	4.0	2.0	20	45-52	0.5	0	0	18
M15	4.0	10.0	2.4	4.0	1.0	20	38-42	0.5	0	0	19,20

*The pH range of 5 to 10 was considered.
†No saturation of any solid in the pH range of 5 to 10

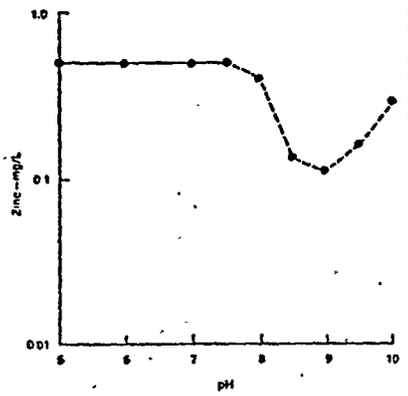

Figure 3. Precipitation diagram for zinc in model system M8

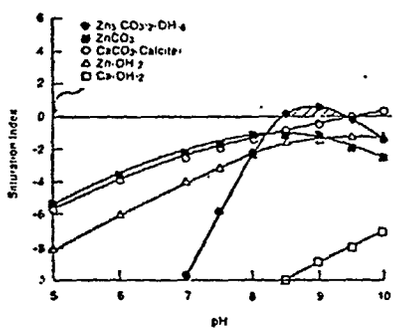

Figure 4. Saturation Index diagram for model system M9

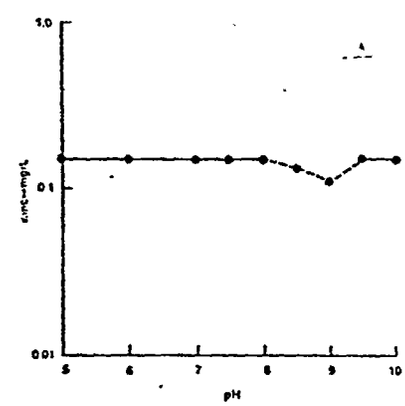

igure 5. Precipitation diagram for zinc in model system M9

IBM 370/168 computer. Tables 3 and 4 summarize the aqueous and solid species considered, and the equilibrium constants employed in the calculations are given in Tables 5 and 6. The temperature was assumed to be 25°C, and the computer program calculated the solution ionic strength based on the equilibrium concentration of charged species. Activity coefficients of uncharged molecules and the activities of water and all solids were assumed to be unity.

The Saturation Index (SI) diagrams were constructed by constraining REDEQL.EPAK to the condition that no solids be permitted to precipitate, even though a state of saturation or supersaturation might exist. The thermodynamic state of saturation was quantified by the SI,[11,30,33] defined as the common logarithm of the ratio of the ion activity product (IAP) to the thermodynamic solubility product constant. As an example, for hydroxyapatite ($Ca_5(PO_4)_3OH$) the mass action equation for which the solubility product constant is defined is

$$Ca_5(PO_4)_3OH(s) = 5Ca^{2+} + 3PO_4^{3-} + OH^- \quad (6)$$

The SI expression is, therefore,

$$SI = \log\left(\frac{a^5Ca^{2+} \cdot a^3PO_4^{3-} \cdot aOH^-}{K_{s0}}\right) \quad (7)$$

When the solid and the solution are exactly in equilibrium, $IAP = K_{s0}$, and $SI = 0$. When the solution is supersaturated with respect to the solid, $IAP > K_{s0}$, and therefore, $SI > 0$. Conversely, when a state of undersaturation exists, $SI < 0$.

The utility of the SI diagrams, consisting of a plot of SI versus pH, is that the region of positive SI defines a range of pH in which active deposition of a coating is thermodynamically favored. Laboratory and field data can then be used to corroborate the theoretical predictions. Once corroboration is accomplished, the SI diagrams may be applied to new localities and situations to develop treatment programs without extensive (and costly) experimentation. In common with observations made previously concerning the difference between the numerical saturation state of calcium carbonate and the effectiveness of the coating produced, the same limitation can apply to any other precipitated solid with any component(s) indirectly affected by pH.

Another type of diagram was prepared by having the computer program "allow" precipitation of whatever solids became supersaturated at a given pH and then calculate the predicted chemical speciation. By examining the final total concentrations of dissolved forms of various elements and the mass of precipitated solid, minimum treatment dosages may be estimated by selecting concentrations that exceed the equilibrium solubility level, providing that the thermodynamic equilibrium constants are not in error, and that the system can be characterized by equilibrium thermodynamics. Figures 1-20 present SI and associated precipitation diagrams for eleven of the model systems summarized in Table 7.* The model systems are correlated with the DWRD experimental studies (Table 8).

Obviously, a degree of uncertainty must be attached to each calculation of SI or equilibrium-soluble concentration of zinc, calcium, or orthophosphate shown in the diagrams. Since the computer models depend on the results from a combination of many equilibrium constants interacting as a group, only semiquantitative conclusions should be drawn unless correlation with detailed field or laboratory data suggests that more confidence can be placed in the predictions. An analysis by Langmuir[11] of the sizes of errors generated in the calculation of saturation indexes of calcite and dolomite ($CaMg(CO_3)_2$) from carefully collected and analyzed geochemical field data indicates a probable uncertainty of ±0.1 SI unit. The experience of the authors has been that the quality of the data from most environmental systems is greatly inferior, and an uncertainty of ±0.5 SI unit is conservative. The uncertainty is even greater when redox reactions are involved or when the solubility constants are poorly known. Major sources of poor data include pH measurements, lack of differentiation of dissolved versus suspended forms for metals (particularly for such elements as iron, manganese, and lead), poor means of estimation of the redox potential (Eh, pE, and so on) of the water, the frequent absence of equilibrium in the case of redox-sensitive species, and poor conversion of alkalinity titration data to total carbonate concentration (or differentiation among the various carbonate species).

Protection by zinc precipitation. Aspects of the geochemistry of zinc have been widely investigated for fresh natural waters and sea water.[23,34-37] Nriagu[38] has studied the solubility of α-hopeite ($Zn_3(PO_4)_2 \cdot 4H_2O$) and some of the equilibria of zinc-orthophosphate complexation. Solubility constants and other thermodynamic data for relevant zinc solids and complexes have been determined or critically reviewed by many investigators.[3,25,39-42]

From the context of metal-removal precipitation, Patterson et al[43] have presented some experimental data interpreted in the framework of the solids $Zn(OH)_2$ and $ZnCO_3$, plus four zinc-hydroxide complexes. Under several of the experimental conditions, however, the solid basic zinc carbonate (also known as zinc hydroxycarbonate, hydrozincite, and

*Diagrams for model systems listed in Table 7 but not illustrated in this paper can be obtained from the senior author.

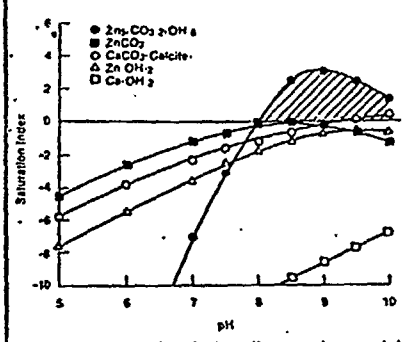

Figure 6. Saturation Index diagram for model system M10

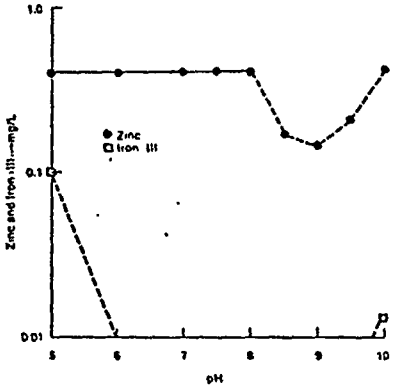

Figure 9. Precipitation diagram for zinc and iron (III) in model system M11

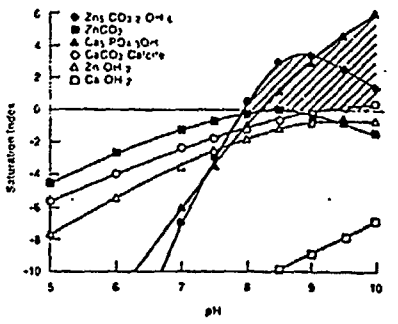

Figure 12. Saturation Index diagram for model system M12P

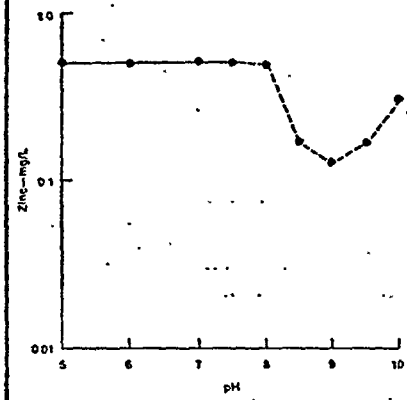

Figure 7. Precipitation diagram for zinc in model system M10

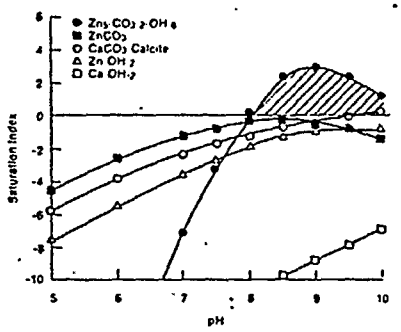

Figure 10. Saturation Index diagram for model system M12

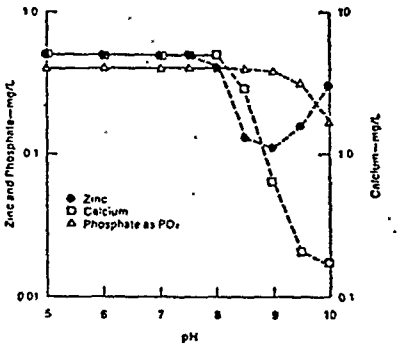

Figure 13. Precipitation diagram for zinc, calcium, and orthophosphate in model system M12P

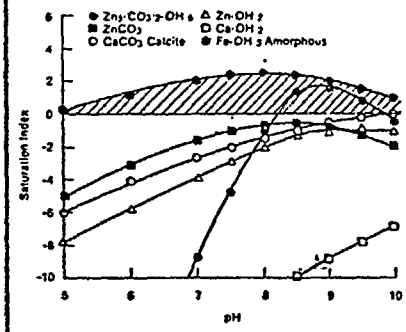

Figure 8. Saturation Index diagram for model system M11

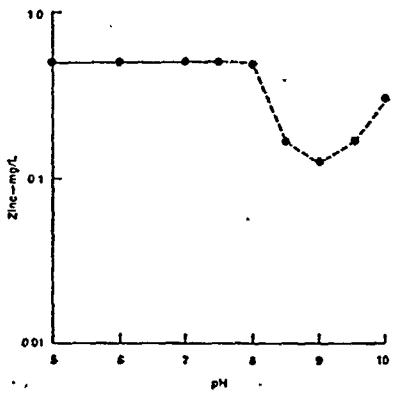

Figure 11. Precipitation diagram for zinc in model system M12

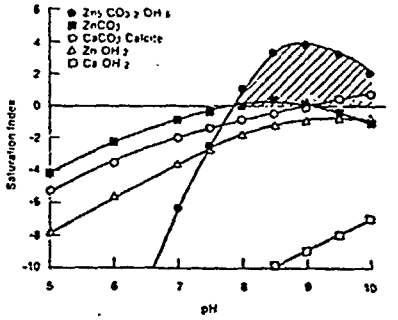

Figure 14. Saturation Index diagram for model system M13

$Zn_5(OH)_6(CO_3)_2$) and zinc-carbonate complexation were probably significant controlling factors also.[28,39,40]

Larson[41] has suggested that hydrozincite may be an effective corrosion inhibitor for galvanized steel piping in the pH range of 7.5 to 8.5 at alkalinities of 50 to 100 mg/L as $CaCO_3$. Mah and Boatman[45] did a limited corrosion-inhibitor study with A-C pipe using a combination of lime and zinc orthophosphate. The zinc level given was 0.3 mg/L, the "lime + orthophosphate" concentration was "5.0 mg/L" (form unspecified), and no other solution parameters (pH or carbonate concentration) were definitively reported. They observed some deposition of zinc and iron, and less apparent leaching of calcium and silicon, but no deposition of phosphorous. The fiber count data were inconclusive.

The results of DWRD experiments 1-5, 11-16, and 19 (Tables 1 and 2) may be compared with the SI and precipitation

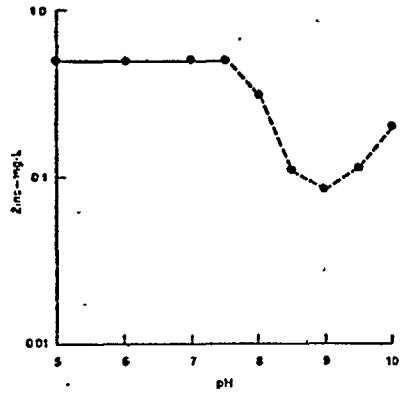

Figure 15. Precipitation diagram for zinc in model system M13

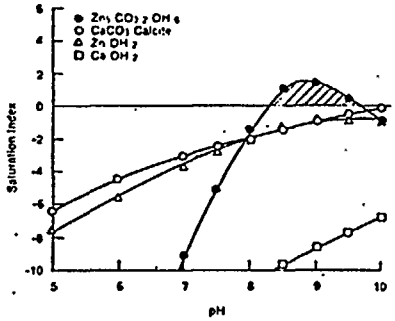

Figure 18. Saturation Index diagram for model system M14

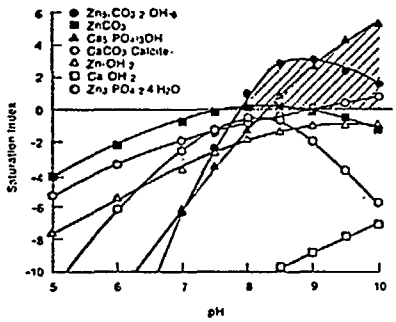

Figure 16. Saturation Index diagram for model system M13P

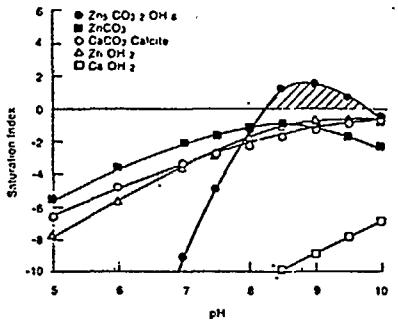

Figure 19. Saturation Index diagram for model system M15

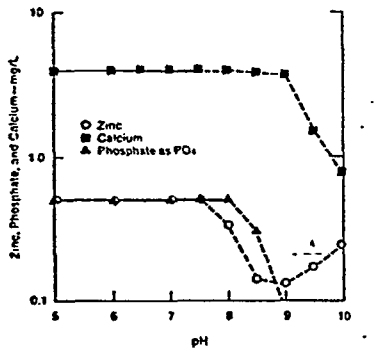

Figure 17. Precipitation diagram for zinc, calcium, and orthophosphate in model system M13P

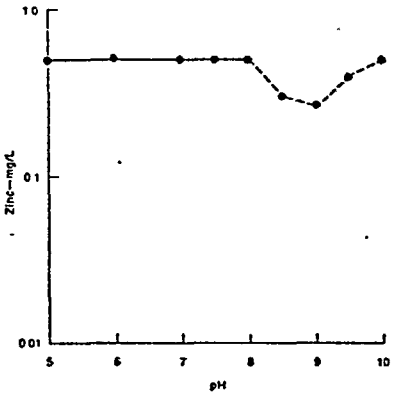

Figure 20. Precipitation diagram for zinc in model system M15

diagrams calculated for the model systems (see Tables 7 and 8).

Monitoring the rate of calcium leaching often gives a good prediction of surficial pipe condition,[2] particularly when used in conjunction with a complete water analysis.

A higher rate of calcium leaching was observed at pH 7.0 than at pH 8.2 in control experiments 1 and 3. Figure 21 shows the effect of 0.3 to 0.6 mg/L zinc added as zinc orthophosphate compared with the untreated equivalent, both at pH 8.2. The solution rate of the calcium-containing cement materials was greatly restricted. Figure 22 indicates, however, that at pH 7.0, after an induction period of about 80 days, the leaching rate of the coupon in the zinc-containing system (experiment 4) was essentially the same as that of the coupon in the control system (experiment 3). Upon inspection, the coupon from experiment 3 was noticeably softened. Experiment 5 (Figure 23) consisted of the substitution of zinc chloride for zinc orthophosphate at pH 8.2; following a very brief induction period, the calcium solution rate was seen to be extremely low. A very hard surficial coating on the coupon was observed when it was removed and inspected.

Experiment 12 consisted of the same quality of water as in experiment 5 at a pH of 7.5 and resulted in a coupon that was noticeably softened. Experiment 16 used zinc sulfate as the zinc source in water similar to that of experiments 2 and 5. The coupon was protected by a hard bluish-grey-colored coating like that from experiments 2 and 5.

The sulfate salt of zinc is interchangeable with the chloride and orthophosphate salts because the formation constants of the sulfate complexes of calcium and most other cations present in a drinking water are small enough that zinc solubility is only significantly affected at unrealistically high sulfate levels.

The experimental observations correlate extremely well with Figures 10-13, which predict an onset of hydrozincite precipitation at a pH of approximately 7.8. Reduction in the zinc levels in the dosed tanks also showed a correlative slowing in rate around 0.3 mg/L in experiments 2 and 5. Virtually no reduction in zinc was noted in experiment 4.

Model system M8 was developed to anticipate the effect of lowering the calcium level in the water, while maintaining the same pH, carbonate level, and zinc dosage. Zinc chloride was chosen for all but one of the remaining experiments because it gave performance equivalent to the orthophosphate salt, and it did not generate the discoloration (microbiological growth) evident at the surface of the O-ring seal around the tank lid (see part 1 for experimental apparatus[2]). The pipe coupon from experiment 11 was covered by a hard grey coating similar to that of coupons from experiments 2 and 5. Figures 2 and 3 predict deposition of a hydrozincite coating, an indication of good protection. The main difference in protection afforded by model systems M8 and M8P versus M12 and M12P is that less protection is theoretically available at extremely high pH in the absence of orthophosphate, as a result of the low calcium-carbonate precipitation potential. The zinc equilibria are clearly dominant (Figures 2, 3, 6-13). The absence of calcium does not detract from the zinc coating process, but its presence is probably desirable to help stabilize the calcium-silicate phases of the portland cement.

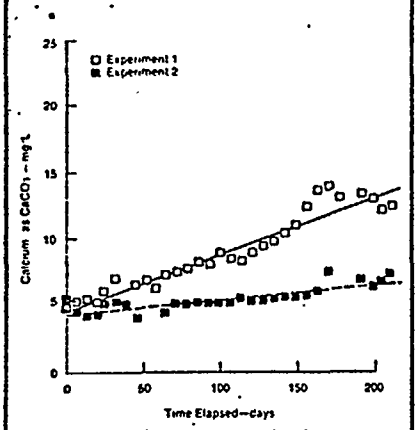

Figure 21. Calcium concentration increases at pH 8.2 during experiment 1 (control) and experiment 2 (zinc orthophosphate treatment)

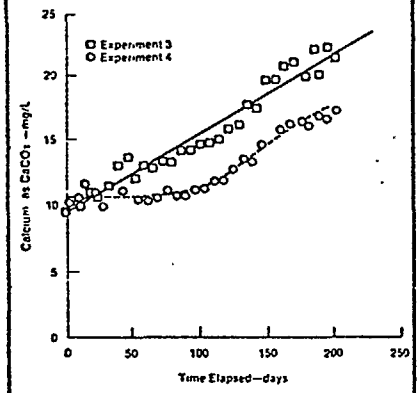

Figure 22. Calcium concentration increases at pH 7.0 during experiment 3 (control) and experiment 4 (zinc orthophosphate treatment)

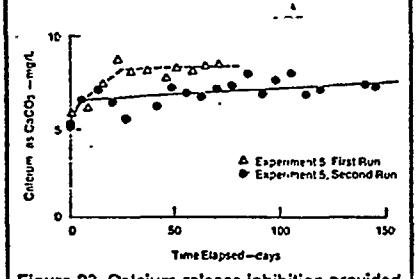

Figure 23. Calcium release inhibition provided by zinc chloride treatment at pH 8.2

Data are successive runs using the same coupon (experiment 5)

Experiment 14 involved a reduction in the carbonate level in the water to approximately 2 mg/L as $CaCO_3$, but an increase in the calcium content to an initial value of 32 mg/L as $CaCO_3$. Substantial calcium leaching was observed for approximately the first 50 days, with a lesser rate following (Figure 24). The decrease in rate is interpreted as the result of the onset of hydrozincite formation after a period of initial leaching of easily available calcium and the increase in carbonate content. The carbonate increase is attributed to CO_2 absorption from the air. There is a strong correlation among the time of the zinc decrease, the increase of carbonate, and the slowing of the calcium leaching (curves for zinc and total carbonate are not shown). Of the coupons from tests using zinc addition at pH 8.2, this coupon appears less protected than all others, except possibly that from experiment 13. The low level of carbonate puts the system depicted by model M14 and demonstrated by experiment 14 on the threshold of hydrozincite precipitiation (pH ~ 8.3), thereby making the protection by zinc minimal. The protection by calcium-carbonate deposition would also be impossible, even up to pH 10.

The last laboratory zinc-protection experiment to be discussed here is experiment 13, where the zinc concentration was reduced to 0.1 to 0.2 mg/L with calcium and alkalinity levels of 10 to 15 mg/L as $CaCO_3$ and 19 to 21 mg/L as $CaCO_3$, respectively. The coupon was noticeably softened as would be predicted by model system M9 (Figures 4 and 5). The low level of zinc employed was insufficient to provide hydrozincite precipitation protection below a pH of approximately 8.5.

Figure 5 shows clearly that even at a higher pH, very little zinc would be deposited compared with many of the other systems.

The relationship of zinc solubility to total dissolved carbonate concentration and pH is displayed in a slightly different manner by Figure 25. This solubility diagram was constructed considering the aqueous zinc species and zinc solids given in Tables 5 and 6 and the ionic strength. The calculation procedure was essentially the same as that utilized in a previous lead solubility study.[46] One of the significant predictions obvious in this diagram is that little advantage is derived from carbonate concentrations above approximately 50 mg/L as $CaCO_3$ in the pH range of 8 to 9. A pH of 8.5 affords considerably more protection than pH 8.0, but pH 9.0 shows only a small improvement over pH 8.5.

Experiments of long duration at zinc concentrations greater than 0.5 mg/L have not been performed, primarily for three reasons. The first is that the most desirable treatment procedure would be one involving a minimal dosage of added chemicals. Second, there is the possibility of zinc toxicity in fish, which could result if wastewater treatment provided inadequate zinc removal. This possibility is briefly discussed in a later section of this paper. There is no evidence of any danger to humans, however. Third, even if a high dosage is employed by a utility as a conditioning step, the equilibria may be reversible (such as with calcium carbonate) to some extent, and continued dosing at the threshold of hydrozincite saturation would probably be necessary. A test of a one-week dose of zinc at 1 mg/L followed by a lowering of the zinc concentration to 0.3 mg/L (conditions otherwise similar to experiment 2) is presently under way to test the effectiveness of such a procedure. Perhaps only intermittent supplementation of zinc would be possible if the reaction reversibility were slow.

The role of orthophosphate. The role of the orthophosphate in the coating process of the DWRD experiments is apparently minor or nearly irrelevant. The published solubility constants and phase diagrams for zinc orthophosphate[38,47] indicate that these compounds are too soluble to reach a state of supersaturation under any of the conditions of the DWRD laboratory experiments. Additionally, supersaturation is not indicated at any of the combinations of pH, zinc, and orthophosphate concentrations of the computer-modeled systems. Evidence is provided by the energy-dispersive x-ray spectrometry data of Mah and Boatman[45] and this laboratory[48] which show that phosphorous is not present on the surface of the pipe samples, but that zinc is. Also, no phosphate decrease in solution was observed within the precision of the analytical method used.

Considerable uncertainty exists in the selection of the proper value for the solubility constant for hydroxyapatite. The precipitation process involved and the exact crystal chemical nature of the solid formed are both highly variable and very sensitive to the experimental conditions employed.[49-52] Lundager Madsen[34] has suggested that although hydroxyapatite possesses only one true thermodynamic solubility constant, it is useful operationally to employ two different solubility constants. One would be used when precipitation is being considered and the other when dissolution processes are contemplated. The value selected in Table 6 reflects a relatively high estimate of hydroxyapatite solubility.

The difficulty in quantitatively describing the calcium-orthophosphate equilibria arises in large part from the tendency for octacalcium phosphate or brushite to be the initially precipitated phase,[50,53,55,56] with the onset of precipitation occurring when their solubility products are exceeded. Subsequently, these

...to hydroxyapatite, though possibly after a very long time.[50,53] A more correct approach may be the use of one of the alternative salts to predict the onset of precipitation. There is also significant evidence of the inhibition of precipitation by low concentrations of carbonate, magnesium, and strontium ions.

In conclusion, concerning the role of orthophosphate, it is unlikely that zinc- or calcium-orthophosphate solids could provide protection of A-C pipe, except possibly at very high pH levels or at extremely high levels of calcium, zinc, or orthophosphate. There was essentially no difference in the hardnesses of the coatings provided by the zinc-chloride systems, the zinc-orthophosphate systems, and the zinc-sulfate system. The ranges of pH, zinc, and carbonate concentrations necessary for A-C pipe protection would be the same for the three zinc salts, because the aqueous orthophosphate complexes are of minor importance in water systems at the dosage levels suggested.

Substitution of other phosphate compounds for the chloride, sulfate, or orthophosphate-zinc salts is not justified on the basis of the experiments reported here. The molecular structure and aqueous chemical behavior of "condensed," "glassy," or "poly" phosphates are quite different from that of the orthophosphates.[49,50] The ability of many of the condensed, glassy, or polyphosphates to form strong aqueous chelates or complexes with Ca^{2+} and Al^{3+}, which are major pipe components, as well as with other potentially protective ions (such as Zn^{2+}, Fe^{2+}, or Mn^{2+}) may enhance the solubility of the pipe under many conditions. Further theoretical and laboratory evaluation of the behavior of the alternate phosphate compounds is necessary before substitution is carried out.

Mechanism of A-C pipe protection by zinc. Positive identification of the exact mechanism involved in the zinc coating process has not been made. However, a two-step mechanism consistent with the laboratory and field data gathered thus far can be postulated. The first step is the attainment of a state of saturation with respect to zinc hydroxycarbonate hydrozincite:

$$5Zn^{2+} + 6OH^- + 2CO_3^{2-} \rightleftharpoons Zn_5(OH)_6(CO_3)_2(s) \quad (8)$$

The zinc levels in the experiments where a coating is formed tend to decrease to values in close agreement with equilibrium total-aqueous-zinc concentrations predicted by the computer model. An experiment was set up with no zinc addition, but a section of used galvanized pipe as a zinc source, with water quality otherwise the same as experiment 12. After 40 days the zinc level had risen to 0.3 mg/L, where it remained throughout the final three and a half months of the test. Duplicate samples were filtered by using an all-plastic support unit, and 0.45-μm polycarbonate membranes showed virtually identical zinc concentrations, indicating that the zinc was entirely in dissolved form. The similar concentrations of zinc attained by precipitation and dissolution experimental approaches support the contention that the solubility of zinc is controlled by zinc hydroxycarbonate, and is both reversible and quantitative.

The major difficulty with using this mechanism by itself is the hardness[57,58] of the surfaces developed on the zinc-protected coupons. In mineral form hydrozincite is considered to have a hardness of 2 to 2.5 on the Moh's hardness scale,[58] which roughly corresponds to a Knoop value range[57,59] of 32 to 80. The observed hardness, which is somewhat difficult to assess because of the thinness of the coating and because of occasional unevenness and porosity of the substrate, is more on the order of 4 on a dried coupon.

Several zinc-silicate minerals have tabulated hardness values comparable to the observed hardness and color of the coupon coatings. Table 9 lists hardness values for several zinc solids. The viability of a conversion of hydrozincite to a zinc silicate coating may be qualitatively tested with some of the existing thermodynamic data[22,24] that is available for willemite (Zn_2SiO_4) and $ZnSiO_3$. Hemimorphite ($Zn_4Si_2O_7(OH)_2 \cdot H_2O$), for which thermodynamic data are scarce, is a very reasonable possibility, based on its occurrence as an alteration product in oxidized zones of zinc ore bodies[57] and in galvanized pipe corrosion.[60] Leggett[61] has described experiments where zinc-silica solids of undetermined form were created by titrating dilute, acidic solutions of monomeric silicic acid and zinc to various pH values. The results are somewhat difficult to quantitatively interpret with certainty, because no effort was made to exclude CO_2 gas from the systems, but the formation of hydrozincite, or smithsonite, or both, is very probable under the experimental conditions reported. The given solubility curves are also quite comparable to the DWRD laboratory data and model systems for the silica-free systems. The concentrations of dissolved silica employed by Leggett (0.001 M in $Si(OH)_4$) were much higher than the concentrations in the DWRD bulk solutions, but they may be comparable to levels attained interstitially upon pipe dissolution.

Gilmour and Kittrick[62] have discussed several zinc-solubility experiments concerning behavior in soil systems, and they concluded that in several cases $Zn_2SiO_4(s)$ could be a viable control on zinc activity when hydrogen sulfide lev-

TABLE 8
Correspondence of model and experimental systems

DWRD Experiment Number	Applicable Model System	SI Diagram (Figure)	Precipitation Diagram (Figure)
1	M12	10*	
2	M12P	12	13
3	M12	10*	
4	M12P	12	13
5	M12	10	11
11	M8	2	3
12	M8	2	3
13	M9	4	5
14	M14	18	
15	M12	10	11
16	M12	10	11

*Ignore fields of zinc-containing solids in the diagrams; the other fields will be changed little.

TABLE 9
Moh's hardness values for several zinc minerals[58]

Common Name	Formula	Hardness
Hydrozincite	$Zn_5(OH)_6(CO_3)_2$	2-2.5
Smithsonite	$ZnCO_3$	5
Willemite	Zn_2SiO_4	5-5.5
Hemimorphite	$Zn_4(Si_2O_7)(OH)_2 \cdot H_2O$	4.5-5
Zincite	ZnO	4-4.5

TABLE 10
Gibbs free energy of formation values at 25°C employed in the construction of the E-pH diagrams in figures 26 and 27

Species	ΔG_f°—cal/mol	Source
H_2O	−56 690.	1
OH^-	−37 604.	1
$H_2CO_3^\circ$	−148 950.	2
HCO_3^-	−140 260.	2
CO_3^{2-}	−126 190.	2
Fe^{2+}	−18 850.	4
$Fe(OH)_2^\circ$	−104 200.	4
$Fe(OH)_3^-$	−146 630.	4
Fe^{3+}	−1060.	4
$FeOH^{2+}$	−54 770.	4
$Fe(OH)_2^+$	−106 700.	4
$Fe(OH)_3^\circ$	−152 600.	4
$Fe(OH)_4^-$	−198 400.	4
$Fe(OH)_3(s)$, fresh ppt.	−164 500.	4
Mn^{2+}	−54 490.	4
Mn^{3+}	−19 700.	4
$MnOH^+$	−96 800.	4
$Mn(OH)_3^-$	−177 900.	4
$MnHCO_3^+$	−197 100.	4
MnO_4^-	−106 900.	4
MnO_4^{2-}	−119 700.	4
$MnO_2(s)$, pyrolousite	−111 400.	4
$Mn_2O_3(s)$, bixbyite	−210 300.	4
$Mn_3O_4(s)$, hausmanite	−305 900.	4
$Mn(OH)_2(s)$, pyrochrosite	−147 300.	4
$Mn(OH)_3(s)$	−181 100.	4
MnOOH (s), manganite	−133 400.	4
$MnCO_3(s)$, rhodochrosite	−195 100.	4
$Cl_2(aq)$	+1650.	3
$HClO^\circ$	−19 100.	3
OCl^-	−8800.	3

Sources:
1. PARKER, V.B. ET AL. Selected Thermochemical Data Compatible with the CODATA Recommendations. NBS NBSIR 75-968 (1976).
2. Calculated from equilibrium constants given by Harned and Davis in *Jour. ACS*, 65:2030 (1943) and by Harned and Scholes in *Jour. ACS*, 63:1706 (1941) for 25°C, with the value for ΔG_f° H_2O from this table.
3. WAGMAN, D.D. ET AL. Selected Values of Chemical Thermodynamic Properties. NBS Tech. Note 270-3 (1968).
4. Calculated from equilibrium constants and equations tabulated by Plummer et al in WATEQF—A FORTRAN IV Version of WATEQ, A Computer Program for Calculating Chemical Equilibrium of Natural Waters. USGS WRI 76-13 (1976), with other values given in this table.

TABLE 11
*Saturation Index calculations for several potentially protective solids**

Water Supply System	pH	Total Alkalinity	Ca	Mg	Fe	Mn	SiO_2	Al[a]	Calcite	Saturation Index[b] $CaCO_3$ppt[c]	Saturation Index[b] $Fe(OH)_3$	Saturation Index[b] MnO_2[d]	Saturation Index[b] Quartz	Detectable Fibers[e]
Multiple samplings														
D	7.8	220	100	NA	0.3[f]	NA	NA	12.5	0.6	0.1	3.3			none
E	9.4	50	17.6	NA	NA[g]	NA	NA	12.7	0.8	0.3	8			none
Ch	8.0	18	4.4	0.7	0.06	0	6	10.3	−1.5	−2.0	2.6			occasional
Jh[h]	6.5	4	2.3	0.5	0.6	0.03	8.7	7.9	−3.9	−4.4	2.0	−2.1	0.2	few
Iz	6.6	7	2.0	0.6	0.11	0.05	7.4	8.1	−3.6	−4.1	1.4	−1.5	0.3	
I3	6.6	23	0.2	2.3	0.19	0.02	14	9.3	−2.5	−3.0	1.6	−1.9	0.5	
I4	6.4	10	7.2	1.7	0.11	0.01	12	8.7	−3.1	−3.6	1.2	−3.0	0.5	
I5	6.6	16	7.9	2.2	0.01	0	12	8.9	−2.7	−3.2	0.4		0.5	
Kh	7.2	76	38	8.1	0.06	0.04	0.4	11.2	−0.9	−1.4	1.5	−0.6	−0.9	NA[i]
Single samplings														
Plant-L	7.3	155	14	2.3	0.22	0.03	51	11.0	−0.8	−1.3	2.5	2.4	0.9	BDL
System-L	7.4	163	14	2.5	0.26	0.03	49	11.1	−0.7	−1.2	2.7	2.8	0.9	NSS
Plant-M	7.6	180	4.0	1.6	0.12	0.06	35	10.9	−0.9	−1.4	2.5	4.0	0.8	1.0
System-M	8.1	185	6.5	0.9	<0.10	0.03	36	11.6	−0.2	−0.8		5.8	0.8	2.3
Plant-N	7.2	17.2	5.3	2.4	1.4	0.05	16	9.6	−2.1	−2.6	3.3	2.2		BDL
System-N	8.3	26.6	9.8	2.0	0.05	0.02	11	11.1	−0.6	−1.1	2.1	6.3	0.3	NSS
Plant-O	8.5	210	2.3	0.5	<0.1	<0.03	15	11.6	−0.2	−0.7			0.4	8.4
System-O	8.4	216	2.8	0.5	<0.1	<0.03	10	11.6	−0.2	−0.7			0.2	26.8
Plant-P	7.1	130	23	8.4	0.24	0.42	60	11.0	−0.8	−1.3	2.4	2.7	1.0	1.5
System-P	7.0	141	25	9.0	3.6	0.46	60	10.9	−0.8	−1.3	3.5	2.4	1.0	NSS

*Temperature is assumed to be 15°C for systems D-K; 25°C for L-P. E was estimated at +0.62 V. Analysis values are mg/L and mg/L as $CaCO_3$ for alkalinity.
Notes: NA—not analyzed; a—Aggressiveness Index = pH + log (AH) (see text); b—Saturation Index = Log (IAP/K_{s0}) (see text); c—fresh phase described by Suarez (1977); d—solubility constant used for pyrolusite; e—millions of fibers per litre for single samplings (NSS—not statistically significant; BDL—below detection limit); f—raw water contained 1.5 mg/L Fe and unspecified Mn; No Mn value given after aeration, filtration, and chlorination; g—sedimentation and filtration reportedly incomplete after ferric sulfate coagulation; h—water analyses were provided by the utility; i—a water blended from the five systems shown is the actual system input, following chlorination; j—inspection of the pipe showed smooth lining on inside.

els are low enough to preclude the formation of ZnS(s). Additionally, in a paper on corrosion inhibition on metal pipes, Lehrman and Shuldener[63] reported the probable formation of a zinc-silicate phase on galvanized iron pipe carrying hot water following a dosage of 8 to 12 mg/L SiO_2.

To calculate the tendency of hydrozincite to convert to willemite or $ZnSiO_3$, equilibrium constants for the following proposed reactions were calculated directly from Gibbs free energy of formation tables by standard procedures,[22-24] using a value of −755 kcal/mol for zinc hydroxycarbonate derived from the equilibrium constant and equation tabulated in Table 6.

$$2Zn_5(OH)_6(CO_3)_2(s) + 5Si(OH)_4^\circ \rightleftharpoons 5Zn_2SiO_4(s) + 4HCO_3^- + 4H^+ + 12H_2O \quad (9)$$

$$Zn_5(OH)_6(CO_3)_2(s) + 5Si(OH)_4^\circ \rightleftharpoons 5ZnSiO_3(s) + 2HCO_3^- + 2H^+ + 11H_2O \quad (10)$$

The equilibrium constants corresponding to reactions 9 and 10 at 25°C are $10^{-16.1}$ and $10^{-15.9}$, respectively. In DWRD experiments 2 and 4 the bicarbonate concentration was approximately $10^{-3.4}$ M. Therefore, for reaction 9 the equilibrium silica concentration would be approximately 0.2 mg/L SiO_2 at pH 7.5 and 0.05 mg/L SiO_2 at pH 8.2. For reaction 10 the concentrations would be 0.002 mg/L SiO_2 at pH 7.5 and 0.001 mg/L SiO_2 at pH 8.2.

These levels of dissolved silica are exceeded by any of the test waters employed, and they should be exceeded to a greater extent by silica concentrations in the interstices and at the coupon surfaces caused by cement dissolution. While the bulk-solution zinc concentrations are obviously not controlled in the experimental time frame by these zinc silicates, conversion of a hydrozincite surficial coating to a zinc silicate is clearly indicated as a distinct possibility.

In addition to the color and hardness of the pipe-coupon coatings, further evidence that some surface reaction does take place is seen by the presence of some grey zinc-compound coating, even on the pH 7.5 coupons, and on those coupons from systems with insufficient zinc for hydrozincite precipitation at pH 8.2. The presence of a large amount of zinc at the pipe surface appears to be a necessary prerequisite for effective development of a hard coating.

Future research will include the use of some surface analysis techniques, such as polarized light microscopy or Raman spectroscopy, to attempt to define more exactly the nature of the coating.

Protection by sodium-metasilicate solution

Two experiments (9 and 10) were performed to determine the efficacy of sodium-metasilicate ($Na_2SiO_3 \cdot 9H_2O$) addition as a protective procedure for A-C pipe. The pipe coupons, representing a silica concentration of 14 to 18 mg/L at a pH of 7.0 and 8.0 under similar calcium and carbonate chemical conditions (see Table 1), were found upon inspection to be clean and not deteriorated. This result is somewhat in contrast to that reported in a Seattle study,[64] but the silica dosages used in the DWRD tests were somewhat higher than those used in the Seattle experiments (approximately 10 mg/L as SiO_2).

The protection of the coupons in the DWRD tests showed a good correlation with the relatively small increase in calcium observed for both experiments.

Scanning-electron-microscope photographs of both coupons in several locations on their surfaces showed similar appearance, with few fibers obvious on the surface. The coupon from the pH 8.2 experiment had a slightly more uniform appearance, but the difference was small.

The protective mechanism provided by the dissolved silica is not known. The concentration is not high enough to favor spontaneous precipitation of amorphous silica, but it is high enough for quartz formation.

There is a possibility that quartz formation may be enhanced by the structures of many of the silicate solids in the portland cement itself.[21] Some cement phases may tend to induce epitaxial growth, providing a mechanism for relatively rapid coating, because the unsupported crystallization of quartz is very slow.[23] X-ray diffraction analyses[65] of surface samples from two different distribution systems having dissolved silica levels between 6 and 14 mg/L SiO_2 indicate the presence of quartz to possibly a

greater degree than would be expected from the cement matrix itself.

Two of the attractive aspects of the sodium-silicate treatment are the possibility of also protecting several types of metal pipes[41,63-66] without the adverse side effects of orthophosphate and the possibility of treatment at a lower pH. Some difficulty is encountered, however, by certain industrial processes[40,66] when appreciable dissolved silica is present in the water, particularly when the water is heated.

Treatment of deteriorated pipe

Several additional experiments involving coupons taken from distribution systems suffering some surficial softening from aggressive water have also been performed or are in progress.

Coupons softened in previous experiments and from use in a distribution system were placed in a test system similar in chemical composition to experiment 2. The coupons did not show appreciable calcium leaching, but the coating formed was not as hard or smooth as on the new pipe coupons. Presently, a test is in progress in which softened samples are placed in a water slightly over-saturated with calcite at pH 8.65.

The results of DWRD experiments conducted thus far and field observations indicate that addition of the corrosion-control compounds tested thus far cannot be relied upon to provide correction of A-C pipe deterioration. If possible, all softened material should be removed to vide a hard, clean surface; this surface t then be maintained by proper water litioning. The feasibility of cement lining of deteriorated A-C pipe is currently being studied. The success of application of corrosion-control chemicals in water distribution systems will depend on the quality of the pipe surface at the time corrosion-control treatment is initiated. The control of microbiological growths through proper disinfection practice is extremely important, and corrosion-control treatment must be operational before pipes are cleaned. Results of DWRD in-situ pipe rehabilitation studies will be reported at a later time.

Natural inhibitory factors

This section discusses several constituents commonly present in drinking water that may serve to inhibit deterioration of the A-C pipe without any special water-treatment procedure. Several metals (such as lead, cadmium, and copper) not discussed in this section could also form protective coatings, but they are comparatively rare and are generally present at very low levels. Therefore, only the most common metals are covered in detail.

Iron and manganese. Two metals frequently present in drinking waters that could provide protection to A-C pipe by virtue of their low solubilities are iron and manganese. In part 1,[2] samples from water systems I and G were reported to have obvious brown coatings largely composed of iron, and the purveyed waters were shown to have minimal or nonquantifiable fiber counts. Pipe sections from the large-scale DWRD experimental pipe loop were also seen to receive a protective iron coating, even at pH 5.5 and total alkalinity of 1 to 3 mg/L $CaCO_3$. Systems D and E discussed in part 1 have water conditions that could favor the formation of iron coatings. Pipe inspections and detailed chemical analyses were not performed, presumably because virtually no fibers were detected in the drinking water samples, and the AI value was above 12 in each case.

At the completion of experiment 19 (see Tables 1 and 2), duplicate 1-L water samples were taken for fiber counts. After months of operation resulting in a calcium-level increase from 9 to 25 mg/L as $CaCO_3$, one of the samples was determined to have 0.45 million fibers per liter, and the fiber level of the other sample was not statistically significant. The presence of 0.1 mg/L of total iron was observed to impart a light coating to the pipe coupon, which served to help bind fibers even though the pipe surface was softened from water attack (as evidenced also by the calcium leaching).

Several water supplies tested by USEPA, but not discussed in detail in part 1, have also shown low or nondetectable fiber levels in spite of having AI values below 10. In at least one case, a manganese-containing solid was found, in addition to that pound in system I.

The general subject of the chemistry of iron in water has been reviewed by Stumm and Morgan,[23] and Hem.[9,67] Many possible reactions of iron in groundwaters have been discussed in some detail by Hem,[67] Hem and Cropper,[68] Langmuir,[69] and Langmuir and Whittimore.[70] The influence of particle size, surface area, and oxidizing conditions on the solid phases formed and the solubility constants involved have also been intensively studied for both ground and surface waters.[70,71] All of these studies can be used to provide a general descriptive model of conditions that would promote the formation of potentially protective coatings on A-C pipe.

Figure 26 is a potential-pH diagram for 0.1- and 1.0-mg/L iron activities in water containing 40 mg/L as $CaCO_3$ dissolved carbonate species activities, constructed using a WATFIV computer program written by Froning et al.[72] The data used to construct this and subsequent E-pH diagrams are given in Table 10. The formation of a ferric-oxyhydroxide precipitate (written as $Fe(OH)_3$) is profoundly influenced by the redox potential of the water involved, as well as hydrogen ion, metallic species, and carbonate species activities. The oxygenation and precipitation processes are also affected to some extent by sulfate ions[73,73] and the carbonate buffer capacity,[74] but these influences will not be included in this qualitative discussion because of their complexity and relatively small impact.

Few studies have been done on the exact redox potentials developed in drinking water, but typical treatment practices such as aeration and disinfection are likely to generate potentials that could near the theoretical stability limit for water,[23,24] depending on the particular oxidant. Ozone has been observed to generate potentials in the range of approximately 850 to 1000 mV at concentrations of 0.5 to 2.8 mg/L.[75] This would be well into the ferric-oxyhydroxide field at pH values anywhere from 5 to 10.8. Experiments successfully oxidizing iron (II) to iron (III) by ozonation have been conducted.[23] Similar results are provided by chlorination, because the species Cl_2 (aq), $HOCl^\circ$ and OCl^- are all strong enough to oxidize iron easily. Such a mechanism has been suggested by Stumm and Morgan.[23] The iron oxidation has also been linked to dechlorination in the distribution system, giving further corroboration.[76]

The combinations of iron concentration, pH, carbonate concentration, and, possibly, organic matter that provide the most effective A-C pipe coatings have not been studied. Laboratory tests performed by DWRD, energy-dispersive spectrometric and electron microscopic examinations of pipe samples, and a few field observations show clearly that the iron coatings often serve to cover and bind fibers to the pipe surface. However, calcium leaching and pipe softening is not prevented in many cases, indicating continuing deterioration of the cement matrix. Increased hardening with time, resulting from the recrystallization of the iron precipiate,[69,70] may be found and would be a logical consequence, provided that the corrosiveness of the water to the portland cement is not too great or the leaching too rapid.

The low solubility of several manganese solids under oxidizing conditions is another theoretically predictable protective mechansism for A-C pipe. The aqueous chemistry of manganese and its oxides is extremely complicated. In addition to the numerous complexation and hydrolysis reactions it can undergo, manganese also has five valence states attainable in natural and drinking waters.[77] Manganese solids may also participate in redox reactions with other metals;[77,78] like iron hydroxides, they can additionally function as strong adsorbers of other trace metals[78] that may also ultimately interact with the pipe surface. The various aspects of the solubility and redox chemistry of manganese have been stu-

pursued in detail here.

A potential-pH diagram for dissolved manganese species activities of 0.05 mg/L and dissolved carbonate species activities of 40 mg/L as $CaCO_3$ is shown in Figure 27. Selecting the proper solids to use in diagram construction is complicated because of the several polymorphs of a given stoichiometry,[23,26] and the possible dominance of metastable solid species.

Oxidation of manganese to form MnO_4^- is reportedly possible by chlorination,[23] as would be predicted by Figure 27, and by ozonation. The formation of MnO_2 by air oxidation is also common.[77]

Feldspathic sand (approximately 45 percent quartz, 21 percent orthoclase feldspar, and 34 percent plagioclase feldspar) has been reported to be capable of oxidizing Mn^{2+} to form solid MnO_2 near pH 8.[79] Whether or not the various silicates present in portland cement could serve in a similar capacity has not been studied.

Because of the general objectionability of manganese in drinking water, no DWRD experiments have been conducted, or are planned, with this metal. At least two localities tested by USEPA do have identifiable manganese coatings on their A-C pipe, and it remains a viable possibility for other locations as yet not closely examined.

Silica. The role silica can play in A-C pipe protection is quite varied. As was discussed in a previous section on the DWRD laboratory experiments, quartz overgrowths or another form of cement solubility stabilization may take place, an occurrence progressively favored as the dissolved silica concentration rises above 6 mg/L. Silica may also combine with other metals directly to some extent to form a coating. A study done by Kato[80] shows significant coprecipitation of 9.3 mg/L silica with hydrated oxides of manganese and iron in the pH range of 5.0 to 8.0. The coprecipitation was observed to increase with pH, temperature, and oxygen content, with iron being the much more effective precipitator. Though the concentrations of iron and manganese were much higher in Kato's study[80] than would be found in drinking water, the mechanism remains plausible for the development of a thin surficial coating on the A-C pipe. Presumably, similar behavior might be observed in the presence of aluminum hydroxide precipitates.

The relationship between dissolved silica and iron is somewhat complicated by the ability of the silica to act both as a sequestering agent and as a precipitator, depending on concentrations and solution conditions. Several studies have attempted to determine the stoichiometry and formation constants of ferric-silicate complexes with mixed success,[81,82] largely because of difficulties with polymerization in the solutions. Dart and Foley[83] determined the use of sodium silicate as an iron and manganese deposition preventor in communities with either iron problems or iron pipe, or both. In their study, where most of the waters had high silica levels (10 to 25 mg/L) to begin with, the silicate showed signs of acting sometimes as a coprecipitator, sometimes as a former of a thin corrosion-reducing film on the pipe surface, and sometimes as a sequestering agent for ferric iron in solution.

Though the exact nature of the silica reactions involving A-C pipe has not been extensively elucidated, the field and laboratory evidence gathered thus far clearly indicates that silica can play an important role in A-C pipe protection.

Analysis of field data. The reliance that has historically been placed on the AI has unfortunately served to focus analytical attention almost solely on pH, alkalinity, and calcium. Thus, very little additional water chemical data are available when correlations among minor constituent equilibria, pipe conditions, and fiber levels in the water are attempted. Some examples of how such additional data can be utilized to predict more accurately the true aggressiveness of a water toward A-C pipe follow, utilizing the SI concept.

Table 11 summarizes analytical data from eleven systems, the first six of which were described in part 1.[2] Systems L,M,N,O, and P are located in the southern and southwestern United States and represent only one sampling event at each plant before chlorination and one location in the distribution system. The SI for five potentially protective solids was calculated using the computer programs WATSPEC2[29] and WATEQF,[26] which derive the total inorganic carbonate concentrations from titration alkalinity analyses correcting for other reactive species. Corrections are also made for complex and ion-pair formation, temperature, ionic strength, and redox potential. In order to calculate the speciation of the electrochemically active elements, it was necessary either to know from measurement or to estimate the redox potential. Because of the absence of such potential measurements, an estimate of +0.62 V was used, in view of the fact that all waters in the distribution systems were chlorinated. Some bias is introduced, therefore, for samples obtained prior to such treatment. In reference to the previous discussion concerning disinfectants, the estimate of +0.62 V is probably low and will therefore provide a conservative estimate of the precipitation tendency of iron and manganese.

The two systems that are nonaggressive on the basis of their AI value (>12) do indeed show an absence of fibers in the water samples. The oversaturation with calcium carbonate is also shown by the SI for various calcium-carbonate polymorphs. However, System D was also very oversaturated with respect to ferric oxyhydroxide, and there is indication that a similar state exists in system E.[2] No data were available for silica or manganese. Because the pipe was not inspected in either case, one cannot be certain to what extent the various factors are individually responsible for the pipe protection.

The actual nonaggressiveness of the other water supplies shown correlates well with both ferric-oxyhydroxide and quartz oversaturation and very little with the AI. Pipe samples from systems G and I have been examined by energy-dispersive x-ray spectrometry[45,65] and show the presence of manganese as well as iron. Manganese may be present as the result of adsorption, or as a solid, because it would take only a small increase in the estimated redox potential of the water to reach, for example, pyrolousite (MnO_2) saturation (see Figure 22) in system I. A

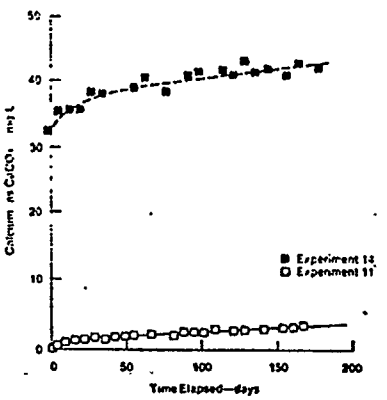

Figure 24. Comparison of calcium leaching at pH 8.2 between a system with high calcium but low carbonate (experiment 14) and a system with low calcium and carbonate at the same level of zinc-chloride addition (experiment 11)

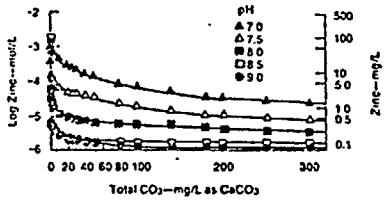

Figure 25. Solubility diagram for zinc versus total inorganic carbonate concentration at fixed pH

$I = 0.005$; 25°C

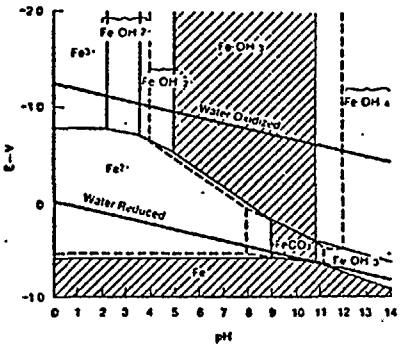

Figure 26. Potential-pH diagram of iron in carbonate-containing water at 25°C

Stability fields are shown for dissolved iron species activities of 0.1 mg/L (——) and 1.0 mg/L (·····). Dissolved carbonate species activities are 40 mg/L as $CaCO_3$. Data are from Table 9.

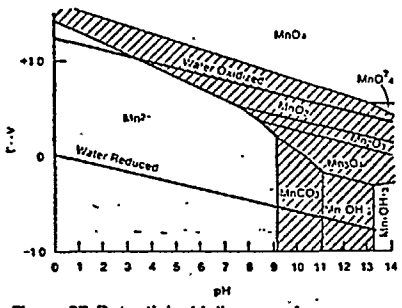

Figure 27. Potential-pH diagram of manganese in carbonate-containing water at 25°C

Stability fields are shown for dissolved manganese species activities of 0.05 mg/L and for dissolved carbonate species activities of 40 mg/L as $CaCO_3$. Data are from Table 9.

similar situation of near-MnO_2 saturation exists for system K, which additionally may derive benefit from the slight ferric-oxyhydroxide oversaturation and the comparatively high level of calcium that may tend to slow calcium-silicate dissolution.

Several interesting trends are apparent in systems L through P. In system O, in spite of the highest AI of the group, some pipe deterioration may have taken place, indicated by the fiber, calcium, and pH increases. The higher true aggressivity of this water is suggested by the low iron and manganese values, the marginal SI of quartz, and the low calcium level. In system P, fibers are actually reduced, possibly resulting from iron precipitation or from a combination of iron and silica. Systems L and P show a large amount of iron and a lesser amount of quartz supersaturation through the system, as well as two of the higher calcium levels of those systems tabulated. Both are significantly undersaturated with respect to calcium carbonate.

The ability of ferric oxyhydroxide to become more insoluble with age[69,71] could be an important factor in the reduction of calcium leaching after many years of service. The existence of a role for organics in the protection observed in these systems has not been studied.

Obviously, more detailed field data must be gathered to test further the accuracy of the predictions of the more comprehensive chemical model of pipe protection presented in this paper. Particular attention should be paid to changes in the various indices during travel in systems as an indicator of active deposition or cement leaching. Correlation with fiber counts and pipe inspections (certainly as important for protected systems as for deteriorated ones) is necessary to define more closely the individual or combinations of chemical factors involved in giving the best prediction of the physical condition of the pipe. The detailed field data and correlations with fiber counts will also serve to define better the water chemical conditions favoring fiber retention over release. The rates and patterns of flow in a distribution sytem may also be of some importance in this regard. The vital need for properly representative samples, carefully preserved and accurately analyzed, cannot be overstressed. The data available are of limited usefulness in rigorous chemical studies, largely because they were not obtained with the aforementioned type of chemical data analysis in mind.

Environmental impact of zinc treatment

The use of zinc orthophosphate for corrosion control in a water distribution system[2] (system G) resulted in the fouling of an industrial filter when zinc concentrations greater than 0.5 mg/L were used. Subsequently, the dosage was reduced to 0.3 mg/L. Because it is necessary to provide a sufficiently high zinc level to cause zinc-hydroxycarbonate supersaturation in order to obtain an effective pipe coating, special provisions may have to be made for or by some water users. In the cited case, some zinc was found to adhere to sections of the pipe at the lower dosage, but the coating was not as well developed as in laboratory studies at the higher zinc level. Recent investigation has shown that zinc levels were substantially reduced during passage through the system and that the precipitation potential of zinc was minimized or even lost entirely. Zinc levels throughout a distribution system must be monitored to assure that zinc-hydroxycarbonate saturation is maintained to the furthest extremities.

Concern must be generated regarding the ultimate fate of the zinc, in view of its potential toxicity to fish and other aquatic organisms. Numerous investigations have been tabulated in this area,[91-99] but research has only occasionally focused on the effect of the zinc speciation. The aqueous forms present have often been shown to be of critical importance in numerous copper toxicity studies.[91]

Conclusions

The experimental field and theoretical data presented combine to suggest several important conclusions with regard to A-C pipe stability and treatment methodologies, in addition to those previously stated.[2]

1. The Aggressiveness Index as traditionally conceived is not theoretically sound from a chemical standpoint to predict fiber release and degradation of the interior pipe surface in systems that are undersaturated with respect to calcite. Fortunately, it has generally proved to predict falsely pipe deterioration more often than to predict falsely pipe stability in field situations. However, an accurate index of A-C pipe condition must take into account the presence of protective constituents such as silica, iron, manganese, and zinc as well as pH, carbonate, calcium, disinfectant concentration, and temperature. The role of organic materials in the protective process still needs investigation, and future field studies need to gather full chemical data to more precisely define the conditions of optimal A-C pipe protection. Observations of A-C pipe sections from many localities conclusively demonstrate that natural inhibitory factors, such as those mentioned, are commonly the pipe protection mechanism, not calcite saturation.

2. Some coating mechanisms serve to bind the asbestos fibers against release but not to seal the cement pipe matrix from dissolution. Thus, calcium and pH increases during flow through a distribution system must be interpreted with caution, as they do not necessarily indicate fiber release. Other chemical reactions in the water may also affect the pH.

3. The chloride, sulfate, and orthophosphate salts of zinc have been tested and found to provide substantial protection of A-C pipe when they are added to the water at the proper concentration and pH ranges and when those chemical conditions are maintained throughout the distribution system. Zinc is the active agent. It acts to coat the pipe and protects the pipe against fiber release and water attack initially by forming a zinc-hydroxy-carbonate precipitate at most carbonate concentrations. Evidence has been presented that the zinc solid then reacts with the pipe surface itself, possibly converting some or all of the coating to a harder zinc-silicate solid phase. The chemical dosages required for a given general water quality are closely estimable by diagrams constructed from computer-assisted calculation of simultaneous aqueous equilibria.

4. When systems involve both metal and A-C pipe, the zinc-chloride and sulfate salts provide little or no protection to the metal pipe. However, DWRD tests at pH 8.2 with lead and A-C pipe in the same recirculation system show that the orthophosphate salt provides corrosion inhibition for both types of piping material because of the action of the orthophosphate ion. The lead solubility in such systems appears to be governed by the formation of lead-orthophosphate (rather than zinc-orthophosphate) compounds, while the A-C pipe is protected, as has been discussed in this paper. Cement linings should behave essentially the same or be even more amenable to zinc coating than the A-C pipe matrix.

5. Substantially softened A-C pipe showing loose fibers, a rough surface caused by considerable calcium and silica leaching, or both, may not be able to be rehabilitated by only in-situ zinc treatment, unless a clean and hard surface free of loose fibers can be restored.

6. Several DWRD tests have indicated corrosion of new galvanized piping can probably be inhibited by the formation of a passivating coating of zinc hydroxycarbonate, which is generally more insoluble than zinc orthophosphate. Therefore, the result of the zinc solubility modeling presented in this paper is applicable to that situation as well.

The levels of orthophosphate necessary to protect other types of piping material, such as ductile iron, have not been studied by DWRD. Detailed studies of lead and galvanized pipe solubility will be reported elsewhere.

In final summary, the results of field, pilot-plant, and theoretical studies show that asbestos-cement pipe can be durable and ensure safe service, provided that certain constraints are placed on the water qualities to be transported. These constraints are a combination of complicated chemical factors that can be predicted by considering the total water chemistry of the system. The term "aggressive water," when it is applied to A-C pipe, needs to be redefined in light of these studies. More field studies encompassing pipe inspections and complete water analyses are needed to improve the definition of truly aggressive waters.

Acknowledgments

The authors wish to thank William Mueller, Carl Shadix, Lou Trombly, Jim Caldwell, Vern Maxon, and William Cushingberry for their analytical chemistry support, plus Robert Canter and Kenneth Thomas for assistance with the A-C coupon studies. They also wish to thank Gary Logsdon and James Symons of USEPA DWRD, Carol H. Tate of JMM Consulting Engineers, and Sara E. Ingle, formerly of the Department of Chemistry, University of Minnesota at Duluth, for thoughtful review of this manuscript. They are also appreciative of the patience of Pat Pierson with an extremely difficult manuscript and are indebted to Joseph C. Jackson, A-C Pipe Producers Assn., for comments on the history and intent of the Aggressiveness Index and to Bryant Mather, US Army Corps of Engineers Waterways Experimental Station, for comments on the behavior of cement and concrete in water.

References

1. A Study of the Problem of Asbestos in Water, Part 2. Jour. *AWWA*, 66:9:1 (Sep. 1974).
2. Buelow, R.W. et al. The Behavior of Asbestos-Cement Pipe Under Various Water Quality Conditions: A Progress Report, Part 1—Experimental Results. Jour. *AWWA*, 72:2:92 (Feb. 1980).
3. Schock, M.R. et al. Evaluation and Control of Asbestos-Cement Pipe Corrosion. EPA 600/D-81-067. NACE Corrosion/81, Toronto, Can. (Apr. 6–10 1980).
4. AWWA Standard for Asbestos-Cement Pressure Pipe, 4 in. Through 24 in., for Water and Other Liquids. AWWA C400-77, Rev. of C400-75, AWWA, Denver, Colo. (1977).
5. Definition of Aggressive Waters. Certain-Teed Products Corp., Valley Forge, Pa. (ca. 1978).
6. Langelier, W.F. The Analytical Control of Anti-Corrosion Water Treatment. Jour. *AWWA*, 28:10:1500 (Oct. 1936).
7. Larson, T.E. & Buswell, A.M. Calcium Carbonate Saturation Index and Alkalinity Interpretation. Jour. *AWWA*, 34:11:1667 (Nov. 1942).
8. Fair, G.M. et al. Water and Wastewater Engineering. Vol. 2. John Wiley & Sons, Inc., New York (1968).
9. Hem, J.D. Study and Interpretation of the Chemical Characteristics of Natural Water. USGS Water-Supply, 1473 (2nd ed., 1970).
10. Troxell, G.E. et al. Composition and Properties of Concrete. McGraw-Hill Book Co., New York (2nd ed., 1968).
11. Langmuir, D. The Geochemistry of Some Carbonate Ground Waters in Central Pennsylvania. Geochim. Cosmochim. Acta, 35:1023 (1971).
12. Jacobson, R.L. & Langmuir, D. Dissociations Constants of Calcite and $CaHCO_3^+$ from 0 to 50°C. Geochim. Cosmochim. Acta, 38:301 (1974).
13. Christ, C.L. et al. Stabilities of Calcite and Aragonite. Jour. Res. USGS, 2:2:175 (Mar.–Apr. 1974).
14. Suarez, D.L. Ion Activity Products of Calcium Carbonate in Waters Below the Root Zone. Soil Sci. Soc. Am. Jour., 41:310 (1977).
15. Wiechers, H.N.S. et al. Lime Treatment of Wastewater: Development and Application of a Simple Graphical Technique for Predicting the Chemical Composition of Lime-Treated Secondary Effluent. Prog. Water Technol., 12:347 (1980).
16. Deer, W.A. et al. An Introduction to the Rock Forming Minerals. Longman Group Limited, London (1966).
17. Krauskopf, K.B. Introduction to Geochemistry. McGraw-Hill Book Co., New York (1967).
18. Kitano, Y. et al. Adsorption of Zinc and Copper Ions on Calcite and Aragonite and Its Influence on the Transformation of Aragonite to Calcite. Geochem. Jour., 10:175 (1976).
19. McCabe, L.J. & Millette, J.R. Health Effects and Prevalence of Asbestos Fibers in Drinking Water. Proc. Ann. Conf. AWWA, San Francisco, Calif. (Jun. 1979).
20. Cooper, R.C. & Cooper, C.W. Public Health Aspects of Asbestos Fibers in Drinking Water. *Jour. AWWA*, 70:6:338 (Jun. 1978).
21. Guide to Compounds of Interest in Cement and Concrete Research. Special Rept. 127. Highway Res. Bd., NRC, NAS, NAE (1972).
22. Wagman, D.D. et al. Selected Values of Chemical Thermodynamic Properties. NBS Techn. Note 270-3. (Jan. 1968).
23. Stumm, W. & Morgan, J.J. Aquatic Chemistry. Wiley-Interscience, New York (1970).
24. Garrels, R.M. & Christ, C.L. Solutions, Minerals, and Equilibria. Freeman, Cooper & Co., San Francisco (1965).
25. Baes, C.F. Jr. & Mesmer, R.E. The Hydrolysis of Cations. Wiley-Interscience, New York (1976).
26. Plummer, L.N. et al. WATEQF: A FORTRAN IV Version of WATEQ, A Computer Program for Calculating Chemical Equilibrium of Natural Waters. USGS Water-Resources Investigations 76-13 (Dec. 1976).
27. Loewenthal, R.E. & Marais, G.R. Carbonate Chemistry of Aquatic Systems: Theory and Application. Ann Arbor Science, Ann Arbor, Mich. (1976).
28. Merrill, D.T. & Sanks, R.L. Corrosion Control by Deposition of $CaCO_3$ Films. AWWA, Denver, Colo. (1978).
29. Schock, M.R. Unpublished WATSPEC program modifications. DWRD, USEPA Cincinnati, Ohio (1979).
30. Wigley, T.M. WATSPEC: A Computer Program for Determining the Equilibrium Speciation of Aqueous Solutions. British Geomorphological Res. Group Techn. Bull. 20. Geo Abstracts Ltd., Univ. of East Anglia, Norwich, England (1977).
31. Ingle, S.E. et al. A User's Guide for REDEQL.EPA, A Computer Program for Chemical Equilibria in Aqueous Systems. EPA-600/3-78-024 (Feb. 1978).
32. Ingle, S.E. et al. REDEQL.EPAK Aqueous Chemical Equilibrium Computer Program. Marine and Freshwater Ecology Branch, Corvallis Envir. Res. Lab., Corvallis, Ore. (1979).
33. Wigley, T.M.L. Ion Pairing and Water Quality Measurements. Can. Jour. Earth Sci., 8:468 (1971).
34. Hem, J.D. Chemistry and Occurrence of Cadmium and Zinc in Surface Water and Groundwater. Water. Res., 8:3:661 (Jun. 1972).
35. Zirino, A. & Healy, M.L. Inorganic Zinc Complexes in Seawater. Limnol. Oceanog., 15:6:956 (Nov. 1970).
36. Zirino, A. & Yamamoto, S. A pH-Dependent Model for the Chemical Speciation of Copper, Zinc, Cadmium, and Lead in Seawater. Limnol. Oceanog., 17:5:661 (Sep. 1972).
37. Mann, A.W. & Deutscher, R.L. Solution

Geochemistry of Lead and Zinc in Water Containing Carbonate, Sulphate and Chloride Ions. *Chem. Geol.*, 29:293 (1980).
38. NRIAGU, J.O. Solubility Equilibrium Constant of α-Hopeite. *Geochim. Cosmochim. Acta*, 37:2357, (Apr. 1973).
39. SCHINDLER, P. ET AL. Loslichkeitsprodukte und Freie Bildungsenthalpien von Zinkoxid, amorphem Zinkhydroxid, β_1-, β_2-, φ-, δ- und ϵ-Zinkydroxid. *Helv. Chim. Acta*, 47:4:982 (1964).
40. SCHINDLER, P. ET AL. Loslichkeitsprodukte und Freie Bildungsenthalpien von $ZnCO_3$ und $Zn_5(OH)_6(CO_3)_2$ bei 25°. *Helv. Chim. Acta*, 52:8:2327 (1969).
41. BILINSKI, H. ET AL. Determination of the Stability Constants of Some Hydroxo and Carbonate Complexes of Pb (II), Cu (II), Cd (II), and Zn (II) in Dilute Solutions by Anodic Stripping Voltammetry and Differential Pulse Polarography. *Anal. Chim. Acta*, 84:157 (1976).
42. SMITH, R.M. & MARTELL, A.E. Critical Stability Constants: V. 4, Inorganic Complexes. Plenum Press, New York (1976).
43. PATTERSON, J.R. ET AL. Carbonate Precipitation for Heavy Metals Pollutants. *Jour. WPCF*, 49:2397 (1971).
44. LARSON, T.E. Corrosion by Domestic Waters. Bull. 59. Illinois State Water Survey, Urbana, Ill. (1977).
45. MAH, M. & BOATMAN, E.S. Scanning and Transmission Electron Microscopy of New and Used Asbestos-Cement Pipe Utilized in the Distribution of Water Supplies. *Scanning Electron Microscopy*, 1:85 (1978).
46. SCHOCK, M.R. Response of Lead Solubility to Dissolved Carbonate in Drinking Water. *Jour. AWWA*, 72:12:704 (1980). Erratum, p. 36 (Mar. 1981).
47. GOLOSHCHAPOV, M.V. & FILATOVA, T.N. The P_2O_5-ZnO-H_2O System. *Russian Jour. of Inorg. Chem.*, 14:3:424 (1969).
48. CLARK, P. ET AL. Unpublished Data. DWRD, USEPA, Cincinnati, Ohio (1979).
49. VAN WAZER, J.R. Phosphorus and Its Compounds. Interscience Publishers, Inc., New York (1958).
50. BROWN, W.E. Solubilities of Phosphates and Other Sparingly, Soluble Compounds. Environmental Phosphorus Handbook. Wiley-Interscience, New York (1971).
51. MCDOWELL, H. ET AL. Solubility of $Ca_5(PO_4)_3OH$ in the System $CA(OH)_2$-H_3PO_4-H_2O at 5, 15, 25, and 37°C. *Jour. Res. NBS*, 81:2&3:273, (Mar.-Jun. 1977).
52. MORENO, E.C. ET AL. Preparation and Solubility of Hydroxyapatite. *Jour. Res. NBS*, 72A:6:773 (Nov.-Dec. 1968).
53. NANCOLLAS, G.H. ET AL. Calcium Phosphates-Speciation, Solubility, and Kinetic Considerations. Ch. 23 in Chemical Modeling in Aqueous Systems. ACS Symposium Series 93. ACS, Washington, D.C. (1979).
54. LUNDAGER MADSEN, H.E. Ionic Concentrations in Calcium Phosphate Solutions. II: The Solubility of Hydroxylapatite in Water or Salt Solutions at 37°C. *Acta Chem. Scand.*, A29:745 (1975).
55. JERVOE, P. & LUNDAGER MADSEN, H.E. Calcium Phosphates with Apatite Structure I: Precipitation at Different Temperatures. *Acta Chem. Scand.*, A28:477 (1974).
56. CORSARO, G. & SUTHERLAND, S. The Formation and Behaviour of Hydroxylapatite. Principles and Applications of Water Chemistry. John Wiley and Sons, New York (1967).
57. SINKANKAS, J. Mineralogy. Van Nostrand Reinhold Co., New York (1964).
58. HURLBUT, C.S. JR. Dana's Manual of Mineralogy. John Wiley and Sons, New York (1971).
59. WEAST, R.C. CRC Handbook of Chemistry and Physics. CRC Press, Cleveland, Ohio (1975).
60. LANE, R.W. ET AL. The Effect of pH on the Silicate Treatment of Hot Water in Galvanized Piping. *Jour. AWWA*, 69:8:457 (Aug. 1977).
61. LEGGETT, G.E. Interaction of Silicic Acid with Copper and Zinc and Chemical Changes of the Precipitates with Aging. *Soil Sci. Soc. Am. Jour.*, 42:263 (1978).
62. GILMOUR, J.T. & KITTRICK, J.A. Solubility and Equilibria of Zinc in a Flooded Soil. *Soil Sci. Soc. Am. Jour.*, 43:890 (1979).
63. LEHRMAN, L. & SCHULDENER, H.L. The Role of Sodium Silicate in Inhibiting Corrosion by Film Formation on Water Piping. *Jour. AWWA*, 43:3:175 (Mar. 1951).
64. Seattle Internal Corrosion Study, Phase II Rept. Kennedy Engineers, Inc., Tacoma, Wash. (1977).
65. X-ray analyses, performed courtesy of the Johns-Manville Corp., Denver, Colo. (1974, 1979).
66. COURCHENE, J.E. & KIRMEYER, G.J. Seattle Internal Corrosion Control Plan—Summary Rept. Proc.. Ann. Conf. AWWA, Atlantic City, N.J. (1978).
67. HEM, J.D. Equilibrium Chemistry of Iron in Ground Water. Principles and Applications of Water Chemistry. John Wiley and Sons, New York (1976).
68. HEM, J.D. & CROPPER, W.H. Survey of Ferrous-Ferric Chemical Equilibria and Redox Potentials. USGS Water Supply Paper 1459-A (1959).
69. LANGMUIR, D. Geochemistry of Iron in a Coastal-Plain Ground Water of the Camden, New Jersey, Area. USGS Prof. Paper 650-C. (1969).
70. LANGMUIR, D. & WHITTEMORE, D.O. Variations in the Stability of Precipitated Ferric Hydroxides. Nonequilibrium Systems in Natural Water Chemistry (J.D. Hem, editor). ACS, Washington, D.C. (1971).
71. WHITTEMORE, D.O. & LANGMUIR, D. The Solubility of Ferric Oxyhydroxides in Natural Waters. *Ground Water*, 13:4 (Jul.-Aug. 1975).
72. FRONING, M.H. ET AL. An Improved Method for Calculation of Potential-pH Diagrams of Metal-Ion-Water Systems by Computer. *Corrosion Sci.*, 16:371 (1976).
73. DOUSMA, J. ET AL. The Influence of Sulfate Ions on the Formation of Iron (III) Oxides. *Jour. Inorg. Nucl. Chem.*, 41:1565 (1979).
74. GHOSH, M.M. Oxygenation of Ferrous Iron (II) in Highly Buffered Waters. Aqueous-Environmental Chemistry of Metals (Alan J. Rubin, editor). Ann Arbon Science, Ann Arbor, Mich. (1974).
75. KATZENELSON, E. ET AL. Inactivation of Viruses and Bacteria by Ozone. Chemistry of Water Supply, Treatment and Distribution (Alan J. Rubin, editor). Ann Arbon Science, Ann Arbor, Mich. (1973).
76. WILLIAMS, D.B. Dechlorination Linked to Corrosion in Water Distribution Systems. Water and Sewage Works, (Mar. 1958).
77. MORGAN, J.J. Chemical Equilibria and Kinetic Properties of Munganese in Natural Waters. Principles and Applications of Water Chemistry (S.D. Faust and J.V. Hunter, editors). John Wiley and Sons, New York (1967).
78. HEM, J.D. Increased Oxidation Rate of Manganese Ions in Contact With Feldspar Grains. USGS Prof. Paper 475-C (1963).
79. HEM, J.D. Redox Processes at Surfaces of Manganese Oxide and Their Effects on Aqueous Metal Ions. *Chem. Geol.*, 21:199 (1978).
80. KATO, K. Behavior of Dissolved Silica in Connection with Oxidation-Reduction Cycle in Lake Water. *Geochem. Jour.*, 3:87 (1969).
81. PORTER, R.A. & WEBER, W.J. JR., The Interaction of Silicic Acid with Iron (III) and Uranyl Ions in Dilute Aqueous Solution. *Jour. Inorg. Nucl. Chem.*, 33:2443 (1971).
82. OLSON, L.L. The Interaction of Fe (III) with $Si(OH)_4$. *Jour. Inorg. Nucl. Chem.*, 35:1977 (1973).
83. DART, J.J. & FOLEY, P.D. Silicate as Fe, Mn Deposition Preventative in Distribution Systems. *Jour. AWWA*, 64:4:244 (Apr. 1972).
84. HOOVER, T.B. Inorganic Species in Water: Ecological Significance and Analytical Needs (A Literature Review). EPA-600/3-78-064 (Jul. 1978).
85. Quality Criteria for Water. USEPA, Washington, D.C. (Jul. 1976).
86. WEATHERLY, A.H. ET AL. Zinc Pollution and the Ecology of the Freshwater Environment: Zinc in the Environment, Part I. Ecological Cycling (J.O. Nriagu, editor). Wiley-Interscience, New York (1980).
87. BROWN, V.M. ET AL. Aspects of Water Quality and the Toxicity of Copper to Rainbow Trout Water. *Research*, 8:797 (1974).
88. PAGENKOPF, G.K. Zinc Speciation and Toxicity to Fishes, Toxicity to Biota of Metal Forms in Natural Water. Proc. Workshop, Duluth, Minn. (Oct. 1975).
89. SMITH, M.J. & HEATH, A.G. Acute Toxicity of Copper, Chromate, Zinc, and Cyanide to Freshwater Fish: Effect of Different Temperatures. *Bull. Envir. Contam. Toxicol.*, 22:113 (1979).
90. CHAPMAN, G.A. Effects of Continuous Zinc Exposure on Sockeye Salmon During Adult-to-Smolt Freshwater Residency. *Trans. Am. Fish Sci.*, 107:6:828 (Jun. 1978).
91. MAGNUSON, V.R. ET AL. Relationships of Activities of Metal-Ligand Species to Aquatic Toxicity. Chemical Modeling in Aqueous Systems (Everett A. Jenne, editor). ACS Symposium Series 93. ACS, Washington, D.C. (1979).

Michael R. Schock is a research chemist with and Ralph W. Buelow is retired from the Drinking Water Research Division, US Environmental Protection Agency, Cincinnati, OH 45268.